Author Version: Journal of Geophysical Research: Oceans, vol.122(5);2017; 3753-3770

Spatial variability of upper ocean POC exportin the Bay of Bengal and the Indian Ocean determined using particle-reactive ^{234}Th

S. Subha Anand[1], R. Rengarajan[1], V. V. S. S. Sarma[2], A. K. Sudheer[1], R. Bhushan[1] and S. K. Singh[1]

[1] Geosciences Division, Physical Research Laboratory, Ahmedabad-380009, India
[2] CSIR-National Institute of Oceanography, Regional Centre,176 Lawsons Bay Colony, Visakhapatnam 530017, India

Revised and submitted to
Journal of Geophysical Research: Oceans
(March9, 2017)

Corresponding author: R. Rengarajan (rajan@prl.res.in) Tel: +91 79 26314314

Key points

1. The ^{234}Th based particulate organic carbon export fluxes showed high values in the equatorial Indian Ocean.
2. On the other hand, intense remineralization of organic matter reduced carbon export in the Bay of Bengal.
3. Region-specific refinement of models is required to better predict carbon export fluxes from surface productivity.

Abstract

The northern Indian Ocean is globally significant for its seasonally reversing winds, upwelled nutrients, high biological production and expanding oxygen minimum zones. The region acts as sink and source for atmospheric CO_2. However, the efficiency of the biological carbon pump to sequester atmospheric $CO_2$and export particulate organic carbon from the surface is not well known. To quantify the upper ocean carbon export flux and to estimate the efficiency of biological carbon pump in the Bay of Bengal and the Indian Ocean, seawater profiles of total^{234}Th were measured from surface to 300 m depth at 13 stations from 19.9°N to 25.3°S in a transect along 87°E, during spring intermonsoon period (March – April 2014).Results showed enhanced in situ primary production in the equatorial Indian Ocean and the central Bay of Bengal, and varied from 13.2 mmol C m^{-2} d^{-1} to 173.8 mmol C m^{-2} d^{-1}. POC export flux in this region varied from 0 to 7.7mmol C m^{-2} d^{-1}. Though high carbon export flux was found in the equatorial region, remineralization of organic carbon in the surface and sub-surface waters considerably reduced organic carbon export in the Bay of Bengal. Annually recurring anticyclonic eddies enhanced organic carbon utilization and heterotrophy. Oxygen minimum zone developed due to stratification and poor ventilation was intensified by sub-surface remineralization. ^{234}Th-based carbon export fluxes were not comparable with empirical statistical model estimates based on primary production and temperature. Region-specific refinement of model parameters is required to accurately predict POC export fluxes.

Keywords: GEOTRACES, ^{234}Th, POC export flux, Th*E* ratio, Biological carbon pump, Bay of Bengal, Indian Ocean

1. Introduction

The biological carbon pump is the process through which photosynthetically produced organic carbon in the ocean is exported from the surface to depth by a combination of sinking particles, advection or vertical mixing of dissolved organic carbon and transport by marine organisms (Turner, 2015).It plays a key role in the global carbon cycle by pumping atmospheric carbon dioxide into the deep ocean. Efficiency of the biological carbon pump is determined by the ratio of the amount of particulate organic carbon sinking from the surface to that produced. Most of the organic carbon produced in the ocean's surface is acted upon by microbes and remineralized in the sub-surface waters forming oxygen minimum zones. Mean global ocean net primary production of 58 ± 7 Pg C yr^{-1} (Buitenhuis et al., 2013) and export production of 6 Pg C yr^{-1} (Siegel et al., 2014) revealed that < 5-10 % of the global primary production is exported down from the euphotic zone.

^{234}Th ($t_{1/2}$=24.1 d)is the particle-reactive daughter nuclide of ^{238}U ($t_{1/2}$=4.468x10^9y), which is highly soluble in seawater. Due to the long half-life of ^{238}U relative to ^{234}Th, the two isotopes are in secular equilibrium when there are no net removal or addition processes acting on these species. Particles in the surface ocean mostly from biological production scavenge ^{234}Th. If these particles sink to deeper depths on timescales faster than ^{234}Th in-growth, a deficit of ^{234}Th relative to ^{238}U in the upper ocean is established. The flux of POC is estimated from the ^{234}Thdeficit and the POC/^{234}Th ratio of settling particles. Buesseler et al.(1998)made a global comparison of export production to total production measured by ^{234}Th(known as Th*E*ratio) and found an export of <5 to 10%during non-bloom periods. The model-generated global mean data and the measurement made by ^{234}Th technique is comparable. Comparison of global observations and models include data collected from the Pacific,Atlantic, Southern, Arctic Ocean and the Weddell Sea but unfortunately not many in-situ ^{234}Th measurements were made in the Indian Ocean except a few in the Arabian Sea (Buesseler et al., 1998).

Measurement of particle export can be done following directly with sediment traps and indirect estimates from ^{15}N isotope addition techniques and approaches using export rates of particle-reactive radionuclides such as ^{234}Th, ^{210}Po, ^{210}Pb (Fischer et al., 1988;Friedrich and Rutgers van der Loeff, 2002; Kumar et al., 2004).The role of the Indian Ocean in global carbon export is not clearly understood. Buesseler et al. (1998)measured carbon export in the Arabian Sea, western basin of the northern Indian Oceanby ^{234}Th technique and reported Th*E* ratio between 0.011 and 0.279. In the last decade, new attempt was made to estimate carbon export through new production using ^{15}N isotope addition techniquein the Bay of Bengal and was found to be 35.6 mmol Cm^{-2} d^{-1} (Kumar et

al., 2004).Previous studies reported export production (from new production based on Eppley and Peterson, 1979) in the Indian Ocean by various methods like ^{15}Nisotope addition technique in the Arabian Sea and the Bay of Bengal (Owens et al., 1993; Watts and Owens, 1999; McCarthy et al., 1999;Sambrotto, 2001;Kumar et al., 2004; Prakash et al., 2008) besides by sediment trap method in the Arabian Sea and in the Bay of Bengal (Nair et al., 1999; Ittekkot et al., 1991; Unger et al., 2003). New production to total production ratio(*f*-ratio) estimated by^{15}N isotope addition technique varied widely from 0.03 to 0.9. The *f*-ratio based on organic carbon flux measured by sediment trap method was found to vary from 0.053 to 0.066 in the Arabian Sea and 0.04 to 0.088 in the Bay of Bengal. Comparison of particulate organic carbon export flux measured by ^{234}Th and other techniques varied by a factor of >3. The assumptions, advantages and disadvantages of the methods mentioned above are discussed in great detail by Buesseleret al. (1998);Gruber (2004); and Yool et al. (2007). ^{234}Th based POC export flux measurements in the Bay of Bengal and the Indian Ocean, however, have not been reported thus far. Here we present results of the first^{234}Thbased POC export flux from the Indian Ocean between 20°N and 25.3°S, along a transect of 87°E undertaken as a part of the Indian GEOTRACES program during spring intermonsoon period (March-April 2014) in order to understand the spatial variability and the efficiency of biological carbon pump in sequestering atmospheric CO_2over this region.

2. Sampling and Methods

2.1 Study Area

The Indian Ocean is surrounded by oceans on three sides and by landmass in the north and globally significant due tothe seasonally reversing winds and surface currents. The northern Indian Ocean (5-23°N) comprises of the Arabian Sea in the west and the Bay of Bengal in the east. In comparison with the northern Indian Ocean, equatorial and southern Indian Oceans are oligotrophic in nature. Unlike the equatorial Pacific and the Atlantic Oceans, equatorial Indian Ocean is considered to be a weak upwelling zone due to convergence of trade winds. However, vertical displacement of thermocline, sudden short weather events like cyclones and upwelling by rossby waves were found to enhance productivity in this region (Prakash et al., 2015). Fernandes et al.(2008) observed a very low productivity in the equatorial Indian Ocean ranging from 4 to14 mg C m^{-2} d^{-1}.

The Bay of Bengal forms a part of the north-east Indian Ocean and the eastern boundary of the Indian peninsula extending from 5°N to 21°N and 80°E to 90°E. It is influenced by strong seasonally reversing winds, the Southwest winds (bringing Southwest Monsoon) during June to September and the Northeast winds (bringing Northeast Monsoon) during November-February. A

number of rivers drain into the Bay of Bengal with maximum discharge during peak Southwest Monsoon while Northeast Monsoon brings rainfall only to regions along the east coast of India. In addition to the monsoonal rivers, there are perennial rivers that originate in the Himalaya and drain throughout the year into the bay. The basin receives freshwater of ~1.6 x 10^{12} m^3y^{-1}(UNESCO, 1993) with a suspended load of ~1.4 x 10^9tons,thus forming the largest sediment fan region of the world. High freshwater from rivers spreads as a thin lens on top of high saline seawater developing strong surface stratification, shallow mixed layer depth and warm SST. Despite high freshwater input with more nutrient loadings, the region is considered to be less productive (Kumar et al., 2002). A few other studies showed that the bay acts as a net sink for atmospheric CO_2 (Kumar et al., 1996). Total productivity in the Bay of Bengal varied from 154-975 mg C m^{-2} d^{-1} during April-May with an average new production of 284 mg C m^{-2} d^{-1} (Kumar et al., 2004).

2.2 Satellite Data

Sea surface features including sea surface height (SSH) and Geostrophic currents in the study region were obtained from satellite observations. The merged weekly averaged SSH and derived geostrophic currents were downloaded from US National Oceanic and Atmospheric Administration(NOAA) websites (http://oceanwatch.pifsc.noaa.gov/las/servlets/dataset; http://pathfinder.nodc.noaa.gov) using AVHRR PFV5.2 data (Casey et al., 2010).

2.3. Sample Collection

Seawater samples were collected in the Bay of Bengal and the Indian Ocean as a part of Indian GEOTRACES program in a cruiseonboard ORV SagarKanya (Cruise No. SK 311) from Chennai, India and headed towards the northern Bay of Bengal (19.9°N) beforemoving down along87°E transect towards Port Louis, Mauritius (Fig. 1). Sampling was carried out during spring inter-monsoon period (March 26 – April 23, 2014), stations were located at 2° intervals in the Bay of Bengal, at 3° intervals towards the equatorial Indian Ocean and at distal intervals to the south of equator. We have measured thirteen seawater profiles fortotal ^{234}Th (particulate + dissolved) in the upperocean (0-300 m depth) to estimate the carbon export efficiency of the Bay of Bengal and the Indian Ocean. Vertical profiles of salinity, temperature, dissolved oxygen, fluorescence were measured insitu using sensors attached to clean ultra-trace metal free CTD-Rosette system (SeaBird, USA). High resolution samplingwas carried out by collecting seawater samples at 9 depths between surface and 300 m depth (Fig. 1). Nutrient concentrations were measured by the colorimetric technique following Grasshoff et al. (1992). Complete details (sampling location, water sampling depths, total water column depth, date) of samplescollected for total ^{234}Thare given in Table 1.

2.3.1.Processing and analysis of sample for Total ^{234}Th

For ^{234}Th measurements, a total of 122 seawater samples were collected from 13 stations (11 depths/station) and 5 deep samples from 2000 m depth at selected stations. Sample processing and measurement of ^{234}Th was based on the small-volume technique originally described byBuesseler et al. (2001),Cai et al. (2006) and Martin et al. (2013). About 4 L of seawater sample from required depth was immediately sub-sampled from 12 L Niskinwater samplers into a 4 L Nalgene™ fluorinated narrow-mouth HDPE bottle and acidified using 5 mL of 7.5 M HNO_3. Subsequently, 250 µL of ^{230}Th spike (30.7 ± 0.9 dpm mL^{-1}) was added to each sample and allowed to equilibrate for ~ 8 hrs. After equilibration, pH of the sample was raised to 8.2 using ammonia solution. To this,250 µL of $KMnO_4$ (3.0 g L^{-1})followed by 250 µL of $MnCl_2$(8.0 g $MnCl_2.4H_2O$ L^{-1})were added and mixed well. Samples were kept in a water bath at 60°C for 3 hrs. After cooling, the samples were filtered on a pre-combusted 25 mm (diameter) Whatman™ quartz filter and dried in a hot air oven at 60°C for 8 hrs. Dried samples were removed and mounted on a pre-cleaned plastic holder covered with a thin layer of mylar and aluminum foil (8.0 mg cm^{-2}). Samples were immediately countedonboard using aRISØ GM-25-5A anti-coincidence beta counting system (DTU Nutech, Denmark) to record the initial counts of ^{234}Th from ^{234}Pa. Each sample was counted for 700 min. (7 cycles, 100 min. each). After 6 months, the samples were recounted to determine the background counts from the plastic mounts and MnO_2 precipitate.

To test the performance and efficiencyof the detectors,^{99}Tc standards (high activity standards supplied with the counters) were counted onboard at the beginning and at the end of the cruise. Identical standards were counted in all the five detectors to check the variability in efficiency between the detectors.After final counting, samples were demounted and prepared for ^{230}Th percent recovery and ^{234}Th chemical yield in the MnO_2 precipitate. All the samples were processed by following the methods of Pike et al. (2005). In brief, the MnO_2precipitate was dissolved, spiked with a known weight of ^{229}Th spike (108.19 pg g^{-1} or 51.074 dpm g^{-1}) and equilibrated. Column chemistry was performed to purify Th from other elements and the final solution was prepared in 0.4 M HNO_3. Ratio of ^{229}Th/^{230}Th was determined by using XSERIES 2Quadrupole ICP-MS (Thermo Scientific, Germany).Although there were a few samples with low yields, ^{230}Th recoveries were generally found to be high and stable (92.4 ± 4.7%, n = 108). Measurements of seawater samples from 2000 m depth (Table 2) showed an average ^{234}Th/^{238}U A.R. of 1.014± 0.040 (n=5). ^{238}U was estimated from salinity using the following relationship (Martin et al., 2013):

$$^{238}U\ (dpm\ L^{-1}) = 0.0713 \times salinity \pm 3\% \qquad 1$$

The associated uncertainty is in the vicinity of ±3% and was included when propagating the error related to total ^{234}Th activities. A difference of ≤ 3% in ^{238}U activity is found while using the ^{238}U-salinity relationship given by Owens et al. (2011). The ^{234}Th activity uncertainties were ≤ 3%, which include those uncertainties associated with counting, detector background and calibration and ICP-MS measurements.

2.3.2. POC/^{234}Th in particulate organic matter

For^{234}Thmeasurement in particulate organic matter,8 Lseawater sample was collected at 200 m depth from each station using clean Niskin samplersand filtered immediately,without any processing, onto a pre-combusted 1 µm nominal pore size, 25 mmdia. quartz filter. In general, the POC/^{234}Th ratio gradually decreased with depth which is believed to be associated with preferential remineralization of organic carbon (Buesseler et al., 2006). In addition, the size-fractionated POC/^{234}Th ratio showed greater variation at the surface than at below the euphotic zone (Cai et al., 2006, 2015) and become roughly invariant at 100-200 m depth. Thus use of POC/^{234}Th ratio on particles below euphotic zone will not cause significant error in the calculation of POC export flux. In previous studies, bottle POC/^{234}Th ratios were consistently higher than for large particles (Chen, 2008). It is suggested that the elevated POC/^{234}Th ratio for bottle filtrates may be caused by dissolved organic carbon adsorption and /or preferential capture of living zooplankton with elevated POC/^{234}Th ratios (Buesseler et al., 2006, Cai et al., 2008). The major discrepancies in POC measurements like adsorption of DOC onto filter, small sample volume (~ 1-2 L) and capture of live zooplankton inside Niskin sample bottle were avoided in this study by filtering 8 L seawater onto 25 mm QMA filter (Cai et al., 2008). A study by Sarma et al. (2016) in the Bay of Bengal suggested that stratification significantly influences the input of nutrients to the sunlit zone, resulting in variations in phytoplankton biomass and size structure in the Bay of Bengal. Picoplankton dominate the phytoplankton population in the bay due to limited supply of nutrients and low nutrient requirements. In view of the above the particles were collected using 1 µm quartz filters. After filtration, these samples were dried at 60°C and mounted on pre-cleaned plastic mounts and were beta-counted for initial^{234}Thactivities and later for background corrections. After final counting, the samples wereprepared for organic carbon analysis using a Flash 2000 Organic ElementalCN Analyzer (ThermoFischer Scientific, UK). Prior to analysis, the samples were exposedovernightto HCl acid fumes,to remove inorganic carbon, thendried and packed as small pellets in tin cupsbefore introducing into the combustion tube of the CNanalyzer. Before measurement, the analyzer was calibrated using Low Organic Soil Sample (LOSS) containing 1.65% carbon as standards selected

within the samples' range.Measurement precision of total carbon is determined by repeated measurements of LOSS standards and was found to be ±3%.

2.3.3. POC fluxes derived from ^{234}Th:^{238}U disequilibrium

The ^{234}Th flux scavenged from the upper ocean is estimated from the general equation:

$$\frac{\partial \mathrm{Th}}{\partial \mathrm{t}} = \lambda_{234}(A_{238} - A_{234}) - P + V \quad (1)$$

where, $\frac{\partial \mathrm{Th}}{\partial \mathrm{t}}$ is the change of total ^{234}Th activity with time, A_{238} and A_{234} are activities (dpm L^{-1}) of ^{238}Uand total ^{234}Th, respectively, λ_{234} is the decay constant of ^{234}Th (0.02876 d^{-1}), P is the scavenging rate of ^{234}Th by particles (dpm L^{-1} d^{-1}), V is the sum of advection and diffusion terms.

^{234}Th fluxes (dpm L^{-1} d^{-1}) were calculated by assuming a closed system at steady state:

$$F_{Th} = \lambda_{234} \int_0^z (A_{238} - A_{234}) dz \quad (2)$$

The ^{234}Th: ^{238}U deficits were calculated by integrating the difference between measured total ^{234}Th activities and estimated ^{238}U activities from salinity using the trapezoid approximation of Eq (2). There are different approaches to determine the maximum depth of integration. In the Bay of Bengal, most of the ^{234}Th removed in the surface is released in the sub-surface layers. Considering the depth upto which we obtained prominent ^{234}Th deficit, we have used 100 m as the maximum depth for integration. The POC export flux is calculated using ^{234}Thfluxes multiplied by the ratio of C/^{234}Th on particles. As we have measured C/^{234}Th ratio from particulate matter at a uniform depth of 200 m in all stations, we have used the same for our calculations.

2.3.4. In vitro primary production measurements

The primary production in seawater at different depths in the euphotic zone was measured using enriched sodium bicarbonate ($NaH^{13}CO_3$; 99%; Sigma Aldrich, USA) following procedures as given by Hama et al. (1983). Briefly, ~1 L of seawater sample was taken from different depths in the photic zone in Nalgene transparent bottles and added 1 mL of 2 mM enriched sodium bicarbonate spike and incubated in triplicate light and dark bottles in the deck incubator. The temperature in the incubator was maintained with running water from the seasurface.Different light screens were used to cut the light for the deeper samples. Samples were incubated for 24 h and were filtered through pre-combusted GF/F filters in the same manner as of POC samples. The enrichment of the isotopic composition of the carbon was measured using elemental analyzer coupled to an Isotope ratio mass spectrometer (IRMS; Delta V Plus, Thermo Electron, Germany). The initial isotopic composition of

carbon and nitrogen were measured by filtering the sample soon after addition of spike. The computation of primary production from the concentration of POC and isotopic enrichment were done following Hama et al. (1983). The precision of primary production in terms of the CVwas 5 %.

3. Results

Based on salinity distribution, the study area is distinguished as (i) less saline, highly stratified Bay of Bengal (5°N-20°N) and (ii) high saline, oligotrophic Indian Ocean (5°N- 26°S).The results are described and discussed separately for the Bay of Bengal and the Indian Ocean.

3.1. Bay of Bengal

3.1.1.Spatial variation in hydrographic parameters

Weekly-averaged (March 27to April 24, 2014), mergedsea surface height (SSH) and geostrophic currentsin the Bay of Bengal and the Indian Ocean during the sampling period is shown in Fig. 1a-d. Variationsin merged SSH and geostrophic surface currentsin the Bay of Bengal(Fig. 1a, b)showedan increase inSSH by 50 cm and an associated east-west elongated anticyclonic eddy located close to 18°N. Additionally, two high SSH features and anticyclonic eddieswerealso seen in the southern and western Bay of Bengal. Details of sampling withsalinity and potential temperature at each depth in all the stations are given in Table 1. Salinity in theupper 50 m of the seawater column was low in the Bay of Bengal (north of 10°N)than that of south (Fig. 2a).The salinity difference between surface and 100 m depth was 2.36 in the northof 10°N indicating strong stratification in the Bay of Bengal. The deepening of thermocline and halocline was observed at sta. 3 (Fig. 2) associated with occurrence of anticyclonic eddy (Fig. 1). The high salinity water in the southern bay was also warm compared to the low temperature water in the northern bay (Fig. 2b). The depth of thermocline was shallow (~50 m) in the northern bay (20°N) and deeper towards the south. Though occurrence of the anticyclonic eddy generally increased the thermocline depth, as seen insta. #3 (18°N) in the northern bay, it did not seem to affect the temperature profiles of nearby stations sampled in the bay.Intermittent shoaling of sub-surface waters and thermocline was observed in the study region.Fluorescence peak occurred at the depth above the thermocline (Fig. 2c).It wasatshallow waters (~53 m) in the northern bay (20°N) and deepened(~90 m) towardssouthern bay (8°N).Surface dissolved oxygen concentration (Fig. 2d) showed high values (> 4 mg L^{-1}) from north to south without any significant gradient. The occurrence of oxygen minimum zone (OMZ) was noticed at depth below 100m in the Bay of Bengal (north of equator) and the intensity was increased towards pole. The boundary of the OMZ followed the depth of thermocline. The OMZ was widespread

throughout the sub-surface depths (100 m to ~1500 m) in the Bay of Bengal and the oxygen levels increased in the south of equator. Sectional distribution of dissolved nutrients in the upper 300 m is shown in Fig. 3.

3.1.2. Spatial distribution of ^{234}Th, ^{238}U and ^{234}Th/^{238}U (A.R.)

Depth-latitude-vertical sections of ^{234}Th,^{238}U and ^{234}Th/^{238}U (A.R.) are shown in Fig. 4a-c, respectively andtheir values are presented in Table 1. ^{234}Thactivity varied from 1.66 ± 0.05 to 3.86 ± 0.08 dpm L^{-1} withthe lowestactivity in the north at 18°N(1.66 ± 0.05 dpm L^{-1}) in the Bay of Bengal (Fig. 4a). High ^{234}Th activity (3.86 ± 0.08 dpm L^{-1}) was observed at 300 m in the southern Bay of Bengal (between 11°N and 5°N).The activity of ^{238}U (Fig. 4b) varied from 2.26 ± 0.07 to 2.50 ± 0.07 dpm L^{-1}. The^{234}Th/^{238}U (A.R.)varied from 0.693 ± 0.029 (at 18°N) to 1.548 ± 0.057 (at 11°N). In addition to the high ^{234}Th/^{238}U (A.R.)found at 300 m in the southern Bay of Bengal, high ratio (1.271 ± 0.049)was also seen in the surface waters surrounding the anticyclonic eddy (18°N - 11°N). Individual profiles of ^{234}Th (dpm L^{-1}), ^{238}U (dpm L^{-1}), fluorescence and dissolved oxygen (mg L^{-1}) inall the stations (SK311/1 to SK311/16)are shown in Fig. 5. Due to its conservative property, ^{238}U does not show any significant variability with depth and latitude. Activity of ^{234}Th (black - continuous line) reveals that the activityis low in the photic zone due to its removal by phytoplankton particles as shown in fluorescence peaks (black-dotted line). In contrast to the low activity at the photic zone, sub-surface high activity depicts release of ^{234}Th from particles. The concurrent occurrence of release of ^{234}Th and the decrease in dissolved oxygen (grey - dash lines) shows that the particle remineralisation consumes oxygen in the water column. The disequilibrium between ^{238}U and ^{234}Th at 300 m depth increased from north to south.The stations in the southern Bay of Bengal show high ^{234}Thactivity than ^{238}U indicating more release in the sub-surface depths. Interestingly, the DIN and silicate concentrations were found enhanced at the sub-surface depths where ^{234}Th was found in excess to ^{238}U.

3.1.3. $\delta^{13}C_{POC}$, POC, PP, POC/^{234}Th ratio and fluxes of^{234}Th and POC Export

The δ^{13}C of surface particulate organic carbon ranged between -24.4 and -23.0‰ in the Bay of Bengal. Table 3 shows the spatial variability of POC/^{234}Th ratio, POC Export Fluxes and PP in this study (Fig. 6a-f). ^{234}Th flux integrated down to 100 m was high (1035 dpm $m^{-2}d^{-1}$) at 8°N compared to other stations (0-499 dpm $m^{-2}d^{-1}$).The ^{234}Th fluxes were low and varied between 395 and 499 dpm $m^{-2}d^{-1}$ in the northern Bay of Bengal. In the central bay, which is associated with the outer edges of the anti-cyclonic eddy, particles are either remineralized in the surface and/or sub-surface leading to very low or no ^{234}Th fluxes. POC measured on sinking particles collected at 200 m depth varied

from 0.51 µmol L^{-1} (8°N) to 0.93 µmol L^{-1} (11°N). In northern Bay of Bengal, POC concentration was similar and varied between 0.72 and 0.85 µmol L^{-1}. POC concentration was low in the southern Bay of Bengal (0.51 to 0.65 µmol L^{-1}). Particulate ^{234}Th varied from 0.385± 0.017 to 1.06 ± 0.03dpm L^{-1} with an average of 0.565± 0.02dpm L^{-1} in the Bay of Bengal. POC/^{234}Th ranged from 0.69 ± 0.18 to 2.23 ± 0.12.The estimated POC export fluxes varied from 0.1 to 1.6 mmol C m^{-2} d^{-1}.High export flux (1.6 mmol C m^{-2} d^{-1}) was observed in the northern bay close to Kakinada port (Sta. 1). Integrated column primary production in the Bay of Bengal increased from north (13.2 mmol C m^{-2} d^{-1}) to center (105.1 mmol C m^{-2} d^{-1}) before reducing to 40.6 mmol C m^{-2} d^{-1} in the south. Highest primary production value was near the outer edges of the anticyclonic eddy.It should be noted that the high export in the northern Bay of Bengal occurred in the low primary productive region (Sta. 1, PP=13.9 mmol C m^{-2} d^{-1}).

3.2. Indian Ocean

3.2.1.Spatial variation in hydrographic parameters

Weekly-averaged maps of merged SSH and geostrophic currents shows that the stations located to the north and south of equator (2°N and 3.5°S) were influenced by eastward-moving equatorial currents. In the southern Indian Ocean, due to the influence of sub-tropical thermocline ridge, SSH increased from 35 cm to as high as 85 cm (Fig. 1). The subtropical thermocline ridge is a region located to the south of equator in the western Indian Ocean with high inter-seasonal and inter-annual fluctuations in sea surface properties and SSH, which is attributed toanomalous Ekman convergence along the northern edge of the weakened trades (Webster et al., 1999). Salinity in the Indian Ocean varies from 33.342 to 35.772. Salinity contours (Fig. 2a) show low saline (33.822) waters in the surface of equator and highsaline waters in the sub-surface depths (35.330 at 100 m) of the equatorial Indian Ocean (3.5°S). Salinity in the southern Indian Ocean (25.3°S) was high from surface to 300 m depth (35.197at 4 m to 35.566 at 300 m) compared to equator. Unlike salinity, temperature profiles showed warmer waters (30.237°C) near the equator (2°N) and cooler waters (25.904°C) towards the south (25.3°S). Depth of thermocline increased from equator towards south. Fluorescence maxima followed depth of thermocline (Fig.2). Fluorescence maxima increased from 75 m near equator to 120 m in the southern Indian Ocean (25.3°S).In the sub-surface depths of the equatorial Indian Ocean, high oxic waters (4.8 mg L^{-1}) from the southern Indian Ocean mix with the hypoxic waters (0.2 mg L^{-1}) of the Bay of Bengal.

3.2.2.Spatial distribution of ^{234}Th, ^{238}U and ^{234}Th/^{238}U (A.R.)

Activity of total ^{234}Th is low in the equator and increased towards the southern Indian Ocean. It varied from1.087± 0.051 dpm $L^{-1}$to 2.930 ±0.064 dpm L^{-1}(Table 1). Though remineralization and release of ^{234}Th was not high as found in the Bay of Bengal, significant release was found at Sta. 11, coinciding with the decrease in DO levels in the water column. . ^{238}U activity varied from 2.41 ± 0.07 to 2.55 ± 0.07 dpm L^{-1}. The ^{234}Th/^{238}U (A.R.) varied from 0.725 ± 0.30 to 1.167 ± 0.043 and low ratio was found at 50 m depth in the station (2°N) close to equator. Vertical profiles of ^{234}Th, ^{238}U, fluorescence and dissolved oxygen at each station in the Indian Ocean (SK311-9 to SK311-16) is shown in Fig. 5. The low ^{234}Thactivity in each station is associated with the fluorescence peak. In the deeper depths (~300 m),^{234}Th always shows equilibrium with ^{238}U indicating the absence of intense sub-surface remineralization.

3.2.3. $\delta^{13}C_{POC}$, POC, PP, POC/^{234}Th ratio and fluxes of ^{234}Th and POC Export

The δ^{13}C of surface particulate organic carbon ranged between -24.5 and -23.8‰ in the Indian Ocean. The integrated flux of ^{234}Thvaried from 0 to 1192 dpm $m^{-2}d^{-1}$,the highest flux of ^{234}Thbeing recorded near the equator (2°N). In the southern Indian Ocean,^{234}Th flux decreased from 594 dpm $m^{-2}d^{-1}$(3.5°S) to88 dpm $m^{-2}d^{-1}$ (25.3°S).Concentration of POC varied from 0.45 to 1.78 µmol L^{-1}(Fig. 6b). Particulate ^{234}Th varied from 0.274 to 0.389 dpm L^{-1} with an average of 0.341 dpm L^{-1}. The POC/^{234}Th ratio ranged from 1.47 to 6.48µmol dpm $^{-1}$. High ratio was found at Sta. 9 (2°N) in the more productive equatorial region(Fig. 6d). POC export fluxes ranged between 0 and 7.7 mmol C m^{-2} d^{-1} and showed a decreasing trend from equator to southern Indian Ocean. Carbon export in the Indian Ocean seems highly related to primary production. Primary production in the Indian Ocean ranged from 52.8 to173.8 mmol C m^{-2} d^{-1}. Even though high PP was found at Sta. 10 (3.5°S) thecorresponding POC export was low at 1.0 mmol C m^{-2} d^{-1}.

4. Discussion

Earlier study on^{234}Th based POC export flux in the Indian Ocean region was limited to the Arabian Sea (Buesseler et al., 1998). Thepresent study is the first attempt to estimate the ^{234}Th-based POC export flux in the Indian Ocean, predominantly influenced by freshwater input, salinity stratification, anticyclonic eddies. Spatial variability in POC export and the associated biogeochemical processes occurring in this regionare discussed below.

4.1. Primary Production and ^{234}Th flux

Fernandes and Ramaiah(2016) reported that the Bay of Bengal exhibited net heterotrophy during spring intermonsoon period and low PP along with high bacterial production and high zooplankton

production rendered net heterotrophy in the bay. At times of low autotrophic production, sizeable heterotrophic bacterial biomass and particulates served as source of food for micro- and mesozooplankton. Heterotrophic bacterial productivity (using ^{3}H-Thymidine) incorporation experiments conducted in the bay during spring intermonsoon showed increased bacterial production in the upper 200 m of water column (Ramaiah et al., 2009). Maximum abundance of heterotrophic dinoflagellates and phaeosomes were also found in the Bay of Bengal during this season(Jyothibabu et al., 2006).

Our results shows high PP in the Equatorial Indian Ocean and low PP below this region, whereas Fernandes et al. (2008b) indicated that there doesn't exist a pronounced latitudinal difference in Chlorophyll *a* concentration as well as PP values in the Indian Ocean. Similarly, the bacterial abundances and production rates measured during Southwest Monsoon and Northeast Monsoon in the Equatorial Indian Ocean were found to be lower than those in other regions of the Indian Ocean (Ramaiah et al., 2009). Present study carried out during spring intermonsoon shows that in the Indian Ocean from equator to 25.3°S, there is a decrease in PP by a factor of 3. Kirchman (2000) explained that in the high temperature regimes like the Equatorial Indian Ocean, heterotrophic bacteria utilize the available organic matter (over 70% of PP) and sustains micro- and mesozooplankton biomass. Similarly, in the oligotrophic Southern Indian Ocean, there exists a strong possibility of low PP being utilized by bacteria and transferred to zooplankton before being exported from the upper ocean.

Generally, the primary production in the euphotic zone of the ocean will remove ^{234}Th from the water column with high production leading to more removal and there always exists a positive linear relation between primary production and ^{234}Th removal (Buesseler et al., 1998; Le Moigne et al., 2016). In the Indian Ocean, a positive correlation (r= 0.998; n=3) between primary production and ^{234}Th flux was observed (Fig. 7a). High primary production at Sta. 9 shows very high ^{234}Th removal while at Sta. 10, high production doesn't show corresponding high ^{234}Th flux. Phytoplankton community and ecosystem changes could have altered the net ^{234}Th removal from the seawater. In contrast, a lack of positive relation between primary production and ^{234}Th flux is seen in the Bay of Bengal (Fig. 7b). The ^{234}Th excess with respect to ^{238}U in surface waters (Fig. 5) due to processes such as the surface microbial cycling and the zooplankton grazingas hypothesized by Maiti et al. (2013) would have disturbed the normal relationship leading to insignificant relation between the two. Also there could be phytoplankton blooms being brought by water movement superimposing surface ^{234}Th deficit. On the other hand, a positive correlation between inventory of excess ^{234}Th

with respect to ^{238}U in the upper 100 m water column and PP (r=0.883, n=6, Fig. 7c) is found, thereby confirming that the surface ocean microbial recycling of particulate organic matter.

4.2. POC Export and Export Efficiency in the Bay of Bengal

The POC/^{234}Th ratio in the Bay of Bengal varied in the narrow range between 0.69 ± 0.03 µmol dpm^{-1} and 2.23 ± 0.12 µmol dpm^{-1}(Table 3). These ratios are generally comparable with that measured in the same season in the Arabian Sea (Buesseler et al., 1998), South China Sea (Cai et al., 2008), Southern Ocean and the North Atlantic Ocean (Buesseler et al., 1992, 2001). Buesseler et al. (2006) explained that the high POC/^{234}Th ratio occurs at places with (i) increasing 'Th' ligands in solution, (ii) thehigh volume to surface area ratio in phytoplanktonand (iii) mixed phytoplankton populations with varying volume to surface area. The variation in POC/^{234}Th ratio occurs due to the combination of ^{234}Th decay and remineralization of POC during particle aggregation (Cai et al., 2006c). In this study, Fig. 5 (Sta. 2) showed that at 200 m depth, there is remineralization and release of ^{234}Th suggesting that the degradation of organic carbon would decrease the amount of carbon sinking and ^{234}Th associated with sinking organic carbon. ^{234}Th based POC export flux in the Bay of Bengal measured during spring intermonsoon period varied from 0.1–1.6 mmol C m^{-2} d^{-1} with an average of 0.8 mmol C m^{-2} d^{-1}. Our results are comparable with the POC export flux (0.9 to 6.4 mmol C m^{-2} d^{-1}) in the Arabian Sea– the adjacent basin of the Bay of Bengal (Buesseler et al., 1998), and in the southern South China Sea (3.8 ± 4 mmol C m^{-2} d^{-1}) (Cai et al., 2008). The overall pattern in POC export flux is similar to the patterns found in POC/^{234}Th. High POC export flux was recorded in the northern bay at 19.9 °N. Estimates of new production (^{15}N tracer technique) in the Bay of Bengal during springintermonsoon season showed high new production of 35.8 mmol C m^{-2} d^{-1} (Kumar et al., 2004). This value is 1 - 2 orders of magnitude higher than our value of 0.8 mmol C m^{-2} d^{-1}. Cai et al. (2008) observed that the POC export fluxes calculated from new production is slightly higher than the POC export fluxes derived from the sediment trap or ^{234}Th method. The reasons for this difference are explained by Yool et al. (2007). The primary production in the bay varied from 13.2 to 105.1mmol C m^{-2} d^{-1} with an average value of 51.9 mmol C m^{-2} d^{-1}. The relationship between the POC export and the primary production in Fig. 8 showed low primary production but significant POC export in the northern Bay of Bengal (Sta. 1, coastal station off Kakinada port). At Sta. 3, which wasunder the influence of the anticyclonic eddy, primary productivity and POC export were very low. In the central and the southern Bay of Bengal, PP increased while moving away from land but carbon export remained low. Though Sta. 5 & 6 showed very high PP,there was no resultant carbon export (Table 3). The δ^{13}C of POC ranged between -24.5 and -23‰ in the entire study region

suggesting that most of the organic matter was produced through internal processes and insignificant fraction is contributed by terrestrial sources. Sarma et al. (2016) noticed absence of external sources of nutrients to the Bay of Bengal during non-monsoon period. During non-monsoon season, the reduced river runoff decreased the riverine input of nutrients to the Bay of Bengal. Additionally, the strong salinity stratification significantly influences the input of nutrients to the sunlit zone, resulting in variations in phytoplankton biomass and size structure in the Bay of Bengal. The contribution of microplankton communities is low (10-15%) compared to nano- (20-40%) and picoplankton (50-75%) in the Bay of Bengal (Sarma et al., 2016)during post monsoon period due to strong stratification and less nutrients input. Due to their low density and high surface area to volume ratio, picoplankton and nanoplankton do not sink through the water column and remain suspended in the bay supporting regenerated production. However, the remineralization of sinking coarser fraction occurs at depths below the thermocline and results in the formation of OMZs. As a result, active microbial loop may be operational resulting in dominance of heterotrophy. Dominance of heterotrophy during spring was reported earlier based on oxygen mass balance model (Sarma, 2002). Similarly dominant heterotrophic bacterial abundance of cyanobacteria was also reported in the regions found at the edge of the warm core eddy (Nelson et al., 1985).Th*E*ratio varied from 0.003to 0.117in the Bay of Bengal. The high ratio (Table 3) was obtained for the coastal station off Kakinada port in the northern Bay of Bengal (16.5°N).The Th*E* ratioin the Bay of Bengal were consistent with that from the Arabian Sea (0.011 to 0.089) (Buesseler et al., 1998). Jyothibabu et al. (2006) observed the occurrence of heterotrophic dinoflagellates and cyanobacteria in the Bay of Bengal during spring intermonsoon. The high abundance of smaller phytoplankton, dominated by microbial food web and microzooplankton reduced the vertical flux of biogenic carbon in the Bay of Bengal during spring intermonsoon(Jyothibabu et al., 2008).

4.3. POC Export and Export Efficiency in the Indian Ocean

Measurements made in the Indian Ocean region (2°N to 25.3°S) showed POC/^{234}Thratio varying from 1.39 ± 0.07 µmol dpm^{-1}to 6.48± 0.43 µmol dpm^{-1}. High POC/^{234}Th ratio was found near the equator (2°N) than other regions (3.5°S to 25.3°S) (Table 3). Ourvalues are comparable with the POC/^{234}Thratios reported in the Southern Ocean (Rosengard et al., 2015), Atlantic Ocean (Owens et al., 2015) andthe Arctic Ocean (Cai et al., 2010). Accordingly, POC export flux in theIndian Ocean (2°N –25.3°S) varied from 0.1 ± 0.1 mmol C m^{-2} d^{-1} to 7.7 ± 0.8 mmol C m^{-2} d^{-1} with an average of 2.3 ± 0.3 mmol C m^{-2} d^{-1}. The latitudinal variability observed in carbon export flux from equator to southern Indian Ocean is similar to the changes in the POC/^{234}Th ratio. The carbon export flux in the

same latitude in the Atlantic Ocean varied from 1.9 ± 0.6 to 5.2 ± 1.7 mmol C m^{-2} d^{-1}(mean: 3.0 ± 0.9 mmol C m^{-2} d^{-1}). Interestingly, the carbon export flux near equator (2.6 °S) was high (5.2 ± 1.7 mmol C m^{-2} d^{-1}) in the Atlantic Ocean as well. Primary production in the equatorial Indian Ocean was high (158 to 173.8 mmol C m^{-2} d^{-1}) and decreased significantly in the southern Indian Ocean (71.3 mmol C m^{-2} d^{-1}).A plot of Primary production to carbon export relationship (Fig. 8) shows that 5% carbon is exported in the equatorial Indian Ocean (Sta. 9) while <2% in the southern Indian Ocean. The Th*E* ratio in the Indian Ocean varied from < 0.002 to 0.049 with high (~5%) in the north of equator (2°N). Though primary production is high in the south of equator (3.5°S), the corresponding carbonexport is less in this region

4.4. Comparison of ^{234}Th based carbon export with Modelled flux estimates

There are several empirical models to estimate carbon export using in situ and/or satellite-derived temperature and net primary production or chlorophyll (Laws, 2000; Laws et al., 2011; Dunne et al., 2005; Henson et al., 2011). These models are based on database of in situ measurements which are sparsely distributed in the oceans both spatially and temporally. Laws (2000) and Laws et al. (2011) developed an empirical relation as a function of PP and surface temperature, Tto estimate POC export flux, EF as below:

$$EF_{Laws} = PP \times 0.04756 \times \left(0.78 - \frac{0.43 \times T}{30}\right) \times PP^{0.307} \quad \ldots\ldots(3)$$

Dunne et al. (2005) derived an empirical equation to predict POC export flux as a function of temperature and productivity:

$$EF_{Dunne} = PP \times \left\{-0.0101\ ℃^{-1} \times T + 0.0582 \times ln\left(\frac{PP}{Z_{eu}}\right) + 0.419\right\} \quad \ldots\ldots(4)$$

Henson et al. (2011) got an exponential function using global dataset of only ^{234}Th and trap based export measurements:

$$EF_{Henson} = PP \times 0.23e^{-0.08 \times T} \quad \ldots\ldots(5)$$

We used in situ primary production (PP) and surface temperature (T) to calculate POC export flux estimates from the above three models (Table 3). Here 10 m below the deep chlorophyll maximum (DCM) is taken for the depth of euphotic zone (Z_{eu})(Haskell II et al., 2015). None of the three modelled POC export flux estimates are comparable with values obtained by in situ ^{234}Th based POCfluxes. The above empirical statistical equations to predict export flux as a function of temperature and productivity derived using global dataset may require careful consideration of additional parameters or separate algorithms for different oceanic regimes. Though temperature

dependence of the ecosystem processes provides a dominant control on export flux, factors such as differences in trophic structure, grazing intensity, recycling efficiency, high bacterial activity and associated DOC export are also to be included to accurately predict export fluxes (Maiti et al., 2016).

5. Conclusion

In this study, we utilized $^{234}Th/^{238}U$ disequilibriumto determine POC export from the euphotic zone in the Bay of Bengal and the Indian Ocean during spring inter-monsoon period (March – April, 2014). Our sampling encompassed the salinity stratified Bay of Bengal, outer edges of anti-cyclonic eddy, equatorial and southern Indian Ocean. The highest fluorescence maximum was found in the northern bay (19.9°N) due to more nutrient input from coastal upwelling.Results showed that in the Bay of Bengal, high primary production occurred in the central bay, in the stations located at the outer edges of the eddy but POC export was not high in the central bay as most of the primary produced carbonwas remineralized in the sub-surface depth before being exported to the deep ocean. Dominant heterotrophic conditions in the bay might enhance more remineralization and reduced carbon export. The results reveal that sub-surface remineralization of organic carbon would have intensified the oxygen minimum zone in the Bay of Bengal. The in situ primary productionvaried from 13.2 mmol C m^{-2} d^{-1} to 173.8 mmol C m^{-2} d^{-1}in the Bay of Bengaland the Indian Ocean. The steady state 100 m integrated flux of^{234}Thranged between negligible to 1192 dpm m^{-2} $d^{-1}$and the corresponding POC export flux in this region varied from negligible to 7.7mmol C m^{-2} d^{-1}.Strong stratification and seasonally recurring eddies and equatorial upwelling controls the carbon export to subsurface waters in the Bay of Bengal and equatorial Indian Ocean, respectively whereas low carbon export in the Southern Indian Ocean was caused by weak nutrient supply through vertical mixing. This study suggests that none of the existing models based on empirical statistical equations of temperature and primary production are comparable with in situ measurements of POC fluxes. More studies are required to quantify the seasonal POC export and the role of the Bay of Bengal and the Indian Ocean in global carbon export and CO_2 removal from the atmosphere.

Acknowledgments

This work was funded by Ministry of Earth Sciences, New Delhi. We would like to thank thecaptain and the crew of ORV SagarKanya(SK311) for their assistance in sample collectionduring the cruise. Special thanks to Mr. M. Muruganantham, Pondicherry University, Port Blair for help with sample collection and Dr. J. S. Ray for providing support with QICP MS measurements. Discussionwith Dr. V. S. N Murty, Regional Centre, National Institute of Oceanography, Visakhapatnamwas helpful

toinfereddies using satellite SSH data. Thanks are also due to the GEOTRACES team for jointsampling and data exchange.We would like to thank two anonymous

reviewers for their valuablecomments and suggestions.The data used are listed in the tables. The US National Oceanic and Atmospheric Administration (NOAA) websites (http://oceanwatch.pifsc.noaa.gov/las/servlets/dataset; http://pathfinder.nodc.noaa.gov)is acknowledged for providing SSH and surface current data.

References

Buitenhuis, E.T., T. Hashioka, and C. L. Que´re´(2013), Combined constraints on global ocean primaryproduction using observations and models,*Global Biogeochem. Cy., 27,* 847–858.

Buesseler, K., M. P. Bacon, J. K. Cochran, and H. D. Livingston (1992),Carbon and nitrogen export during the JGOFS North Atlantic bloomexperiment estimated from^{234}Th:^{238}U disequilibria,*Deep Sea Res., PartI,39,* 1115–1137.

Buesseler, K., L. Ball, J. Andrews, C. Benitez-Nelson, R. Belastock,F. Chai, and Y. Chao (1998), Upper ocean export of particulate organic carbon in the Arabian Sea derived from thorium-234,*Deep Sea Res.,Part II, 45,* 2461-2487.

Buesseler, K.O., C. Benitez-Nelson,M.RutgersvanderLoeff,J. Andrews,L. Ball,G. Crossin, and M.A. Charette (2001), Anintercomparisonofsmallandlarge volume techniquesforThorium-234inseawater,*Mar.Chem., 74(1),*15–28.

Buesseler, K.O., C. Benitez-Nelson, S.B. Moran, A. Burd, M. Charette, J.K., Cochran, L. Coppola, N.S. Fisher, S.W. Fowler, W. Gardner, L.D.Guo, O. Gustafsson, C. Lamborg, P. Masque, J.C. Miquel, U. Passow, P.H. Santschi, N. Savoye, G. Stewart, and T. Trull (2006), Anassessmentofparticulateorganic carbon toThorium-234ratiosintheoceanandtheirimpactontheapplication of ^{234}Th asaPOC flux proxy, *Mar. Chem.,100,* 213–233.

Cai. P, M. Dai, D. Lv, and W.Chen (2006a),An improvement in the smallvolumetechnique for determining thorium-234 in seawater,*Mar. Chem., 100,* 282–288.

Cai, P., M. Dai, W. Chen, T. Tang, and K. Zhou (2006b), On the importanceof the decay of^{234}Th in determining size-fractionated C/^{234}Th ratio onmarine particles,*Geophys. Res. Lett.,33* L23602, doi:10.1029/2006GL027792.

Cai, P., M. Dai, W. Chen, T. Tang, and K. Zhou, (2006c), On the importance of the decay of ^{234}Th in determining size-fractionated C/^{234}Th ratio on marine particles, *Geophys. Res. Lett., 33*, L23602, doi:10.1029/ 2006GL027792.

Cai, P.,W. Chen,M. Dai, Z. Wan, D. Wang, Q. Li, T. Tang, and D. Lv (2008), A high resolution study of particle export in the South China Sea based on ^{234}Th:^{238}U disequilibrium, *J. Geophys. Res., 113*,C04019, doi:10.1029/2007JC004268.

Cai, P.,M.RutgersvanderLoeff, I. Stimac, E.-M. Nothig, K. Lepore, and S. B. Moran, (2010), Low export flux of particulate organic carbon in the central Arctic Ocean as revealed by ^{234}Th:^{238}U disequilibrium, *J. Geophys. Res., 115*, C10037, doi: 10.1029/2009JC005595.

Cai, P., D. Zhao, L. Wang, B. Huang, *and* M. Dai *(*2015*)*, Role of particle stock and phytoplankton community structure in regulating particulate organic carbon export in a large marginal sea,*J. Geophys. Res.,* 120, 2063–2095, *doi:*10.1002/2014JC010432.

Casey, K. S., T.B. Brandon, P. Cornillon, and R. Evans, (2010),The Past, Present and Future of the AVHRR Pathfinder SST Program, Pp. 273-287 in *Oceanography from Space: Revisited.* V. Barale, J.F.R. Gower, and L. Alberotanza eds. Springer, http://dx.doi.org/10.1007/978-90-4818681-5_16.

Chen, W., P. Cai, M. Dai, and J. Wei, (2008), ^{234}Th:^{238}U disequilibrium and particulate organic carbon export in the northern South China Sea. *J. Oceanogr., 64*, 417–428.

Dunne, J. P., R. A. Armstrong, A. Gnanadesikan, *and* J. L. Sarmiento(2005), Empirical and mechanistic models for the particle export ratio, *Global Biogeochem. Cy.,19, GB4026, doi:*10.1029/2004GB002390.

Eppley, R. W. and B.J. Peterson(1979), Particulate organic matter flux and planktonic new production in the deep ocean,*Nature, 282*, 677-680.

Fernandes, V. (2008), The effect of semi-permanent eddies on the distribution of mesozooplankton in the central Bay of Bengal, *J. Mar. Res., 4*, 465–488.

Fernandes, V., N. Ramaiah, J. T. Paul, S. Sardessai, R. Jyothibabu,and M. Gauns (2008), Strongvariability in bacterioplankton abundance and production in central and western Bay of Bengal, *Mar. Biol. 153*, 975–985.

Fernandes, V.and N. Ramaiah, (2016), Mesozooplankton production, grazing and respiration in the Bay of Bengal: Implications for net heterotrophy, *J. Sea. Res., 109*, 1-12.

Fisher, N.S., Cochran, J.K., Krishnaswami, S., Livingston,H.D., (1988), Predicting the Oceanic flux of radionuclides onsinking biogenic debris. *Nature 335*, 622–625.

Friedrich, J., van der Loeff, M.R., 2002. A two-tracer (^{210}Po–^{234}Th) approach to distinguish organic carbon and biogenic silica export flux in the Antarctic Circumpolar Current. *Deep Sea Res. II, 49*,101-120.

Grasshoff, K., M. Ehrhardt, and K. Kremling, eds. (1992), *Methods of Seawater Analysis*, Verlag Chemie, Weinheim, 634 pp, http://dx.doi.org/ 10.1002/9783527613984.

Gruber, N.(2004),The dynamics of the marine nitrogen cycle and its influence on atmospheric CO_2, in:*Carbon-Climate Interactions* edited by M. Follows and T. Oguz, Kluwer Academy,Rotterdam, Netherlands, 97-148.

Hama, T., T. Miyazaki, Y. Ogawa, T. Iwakuma, M. Takahashi, A. Otsuki, and S. Ichimura (1983),Measurement of photosynthetic production of a marine phytoplankton population using a stable ^{13}C isotope, *Mar. Biol..,73*, 31-36.

Haskell, II W.Z.,D. Kadko, D. E. Hammond, A. N. Knapp, M. G. Prokopenko, W. M. Berelson, and D. G. Capone (2015), Upwelling velocity and eddy diffusivity from ^{7}Be measurements used to compare vertical nutrient flux to export POC flux in the Eastern Tropical South Pacific, Mar. Chem., 168, 140-150, ISSN 0304-4203, http://dx.doi.org/10.1016/j.marchem.2014.10.004.

Henson, S. A., R. Sanders, E. Madsen, P. J. Morris, F. Le Moigne, and G. D. Quartly (2011), A reduced estimate of the strength of the ocean's biological carbon pump, *Geophys. Res. Lett., 38*, L04606, doi:10.1029/2011GL046735.

Ittekkot, V., R. R. Nair, S. Honjo, V. Ramaswamy, M. Bartsch, S. Manganini, and B. N. Desai (1991), Enhanced particle fluxes in Bay of Bengal induced by injection of fresh water,*Nature*, *351*, 385-387.

Jyothibabu, R., N. V. Madhu, P. A. Maheswaran, C. R. Asha Devi, T. Balasubramanian, K.K.C., Nair, and C. T. Achuthankutty (2006), Environmentally-related seasonal variation in symbiotic associations of heterotrophic dinoflagellates with cyanobacteria in the western Bay of Bengal, *Symbiosis., 42*, 51-58.

Jyothibabu, R., N. V. Madhu, P. A. Maheswaran, K. V. Jayalakshmy, K. K. C. Nair, and C. T. Achuthankutty (2008), Seasonal variation of microzooplankton (20-200 µm) and its possible implications on the vertical carbon flux in the western Bay of Bengal, *Cont. Shelf Res., 28*, 737-755.

Kirchman, D. (2000), Uptake and regeneration of inorganic nutrients by marine heterotrophic bacteria, In*Microbial ecology of the oceans*, John Wiley & Sons, NY, 261–288.

Kumar, M. D., S. W. A. Naqvi, M. D. George, and D. A. Jaykumar (1996), A sink for atmospheric carbon dioxide in the northeast Indian Ocean, *J. Geophys. Res., 101,* C8,18121-18125.

Kumar, S.P., P. M. Muraleedharan, T. G. Prasad, M. Gauns, N. Ramaiah, S. N. deSouza, S. Sardesai,and M. Madhupratap(2002), Why is the Bay of Bengal less productive during summer monsoon compared to the Arabian Sea? *Geophys. Res. Lett., 29*, 2235 doi:10.1029/2002GL016013

Kumar, S., R. Ramesh, S. Sardesai, M. S. Sheshshayee, (2004), High new production in the Bay of Bengal: Possible causes and implications. *Geophys. Res. Lett. 31,* L18304, doi:10.1029/2004GL021005.

Laws, E.A. (2000), Temperature effects on export production in the open ocean,*Global Biogeochem. Cy*., *14*, 1231-1246.

Laws, E.A., E. D'Sa, and P. Naik, (2011), Simple equations to estimate ratios of new or export productionto total production from satellite-derived estimates of sea surface temperatureand primary production. *Limnol. Oceanogr. Meth., 9*, 593–601.

Le Moigne, F. A. C., S. A. Henson, E. Cavan, C. Georges, K. Pabortsava, E. P. Achterberg,E. Ceballos-Romero, M. Zubkov, and R. J. Sanders (2016), What causes the inverse relationship between primary production and export efficiency in the Southern Ocean?, Geophys. Res. Lett., 43, 4457–4466, doi:10.1002/2016GL068480.

Maiti, K., M.A. Charette, et al., (2013), An inverse relationship between production and export efficiency in the Southern Ocean. *Geophys. Res. Lett.*, 40 (8), 1557–1561.

Maiti, K., S. Bosu, E.J. D'Sa, P.L. Adhikari, M. Sutor, K. Longnecker, (2016), Export fluxes in northern Gulf of Mexico - Comparative evaluation of direct, indirect and satellite-based estimates, *Mar. Chem., 184*, 60-77.

Martin, P., M. R. van der Loeff, N. Cassar,P. Vandromme, D. d'Ovidio, L. Stemmann,R. Rengarajan, M.Soares,H. E. González, F. Ebersbach,R. S. Lampitt, R. Sanders, B. A. Barnett,V. Smetacek,and S. W. A Naqvi (2013), Iron fertilization enhanced net community production but not downward particle flux during the Southern Ocean iron fertilization experiment LOHAFEX, *Global Biogeochem. Cy., 27*, 871–881.

McCarthy, J.J., G. Chris,and J. L. Nevins (1999), Nitrogen dynamics during the Arabian Sea Northeast Monsoon, *Deep-Sea Res., II, 46*, 1623-1664.

Nair, R.R., V. Ittekkot, S. J. Manganini, V. Ramaswamy, B. Haake, E.T. Degens, B. N. Desai, and S. Honjo(1999), Increased particle flux to the deep ocean related to monsoons. *Nature*, 338, 749-751.

Nelson, D. M., H. W. Ducklow, G. L. Hitchcock, M. A. Brzezinski, T. J. Cowles, C. Garside, R. W. Gould, T. M. Joyce, C. Langdon, J. J. McCarthy, and C. S. Yentsch, (1985), Distribution and composition of biogenic particulate matter in a Gulf Stream warm-core ring, *Deep Sea Res., PartII, 32(11),* 1347-1369.

Owens, N.J.P., P. H. Burkill, R. F. C. Mantoura, E. M. S. Woodward, I. E. Bellan, J. Aiken, R. J. M. Howland, and C. A. Llewellyn(1993),Size-fractionated primary production and nitrogen assimilation in the northwestern Indian Ocean,*Deep Sea Res., 40(3),* 697-709.

Owens, S.A., K. O. Buesseler, K.W.W. Sims, (2011), Re-evaluating the ^{238}U-salinity relationship in seawater: Implications for the ^{238}U- ^{234}Th disequilibrium method. Mar. Chem., 127, 31-39.

Owens, S.A., S. Pike and K.O. Buesseler, (2015), Thorium-234 as a tracer of particle dynamics and upper ocean export in the Atlantic Ocean. *Deep Sea Res. II, 116*, 42-59.

Pike, S.M., K. O. Buesseler, J. Andrews,and N. Savoye(2005), Quantification of ^{234}Th recovery in small volume seawater samples by inductively coupled plasma mass spectrometry,*J. Radioanalytical Nucl. Chem., 263(2)*, 355–360.

Prakash, S., R. Ramesh, M. S. Sheshshayee, R. M. Dwivedi,and M. Raman (2008), Quantification of new production during a winter Noctillucascintillans bloom in the Arabian Sea,*Geophys. Res. Lett.,35*, doi: 10.1029/2008GL033819.

Prakash, S., R. Ramesh, M. S. Sheshshayee, R. Mohan, and M. Sudhakar(2015), Nitrogen uptake rates and *f*-ratios in the Equatorial and Southern Indian Ocean,*Curr. Sci., 108(2),* 239-245.

Ramaiah, N., V. Fernandes, V. V. Rodrigues, J. T. Paul, and M. Gauns (2009), Bacterioplankton abundance and production in Indian Ocean regions, in *Indian Ocean Biogeochemical Processes and Ecological Variability*edited by J. D. Wiggert, R. R. Hood, S.W. A. Naqvi, K. H. Brink and S. L. Smith, AGU, Washington, D. C., doi: 10.1029/2008GM000711.

Rosengard, S.Z., P. J. Lam, W. M. Balch, M. E. Auro, S. Pike, D. Drapeau, and B. Bowler (2015), Carbon export and transfer to depth across the Southern Ocean Great Calcite Belt, *Biogeosciences., 12*, 3953-3971.

Sambrotto, R.N. (2001), Nitrogen production in the northern Arabian Sea during the Spring Intermonsoon and the Southwest Monsoon seasons,*DeepSea Res, II, 48*, 1173-1198.

Sarma, V.V.S. S.(2002), An evaluation of physical and biogeochemical processes regulating the oxygen minimum zone in the water column of the Bay of Bengal,*Global Biogeochem.Cy.,16(4)*, doi:10.1029/2002GB001920.

Sarma, V.V.S.S., G.D. Rao, R. Viswanadham, C.K. Sherin, J. Salisbury, M.M. Omand, A. Mahadevan, V.S.N. Murty, E.L. Shroyer, M. Baumgartner, and K.M. Stafford. (2016), Effects of freshwater stratification on nutrients, dissolved oxygen, and phytoplankton in the Bay of Bengal, *Oceanogr. 29(2)*, 222–231, http://dx.doi.org/10.5670/oceanog.2016.54.

Siegel, D.A., K. O. Buesseler, S. C. Doney, S. F. Sailley, M. J. Behrenfeld,and P. W. Boyd (2014), Global assessment of ocean carbon export by combining satellite observations and food-web models,*Global Biogeochem. Cy., 28,* 181-196.

Turner,J. T. (2015), Zooplankton fecal pellets, marine snow, phytodetritus and the ocean's biological pump, *Progr. Oceanogr., 130,* 205-248.

UNESCO, (1993),*Discharge of selected rivers of the world,* vol. III. UNESCO, Paris, p. 600.

Unger, D., V. Ittekkot, P. Schafer, J. Tiemann,and S. Reschke(2003), Seasonality and interannual variability of particle fluxes to the deep Bay of Bengal: Influence of riverine input and oceanographic processes,*Deep Sea Res., II,* 50, 897-923.

Watts, L.J., and N. J. P. Owens(1999), Nitrogen assimilation and the *f*-ratio in the northwestern Indian Ocean during and intermonsoon period,*Deep-Sea Res. II,* 46, 725-743.

Webster, P. J., A. M. Moore, J. P.Loschnigg, R. R. Leben, (1999), Coupled ocean-atmosphere dynamics in the Indian Oceanduring 1997–98. *Nature, 401,* 356–359.

Yool, A., A. P. Martin, C. Fernandez, and D. Clark (2007), The significance of nitrification for oceanic new production,*Nature, 447,* 999-1002.

Figure Captions

Figure 1. Weekly averaged mapsof merged AVISO & NIILER sea surface height (SSH) in cm and geostrophic currents in cm s^{-1} (Mar 27-Apr 24, 2014) in the study region with station numbers and sampling locations of GEOTRACES SK-311cruise (a-d). Seawater samples were collected for total ^{234}Th measurements from 13 stations in the Bay of Bengal and the IndianOcean, from 19.9°N to 25.3°Salong 87°E during March-April 2014. Except stations1& 2, all the other stations were located in the open ocean. Samplingfrequency was every 2° interval in the Bay of Bengal and every 3° interval towards equator. Tothe south of equator, samples were collected at distal intervals.

Figure 2. Depth-latitude vertical sections of (a) salinity, (b) temperature, (c) fluorescence and(d) dissolved oxygen in the upper 300 m of the water column of the cruise track.

Figure 3. Depth-latitude vertical sections of (a) DIN, (b) phosphate and (c) silicate in the upper 300 m water column of the cruise track.

Figure 4. Depth-latitude vertical sections of (a) ^{234}Th, (b) ^{238}U and (c) ^{234}Th/^{238}U (A.R.) in the upper 300 m water columnof the cruise track.

Figure 5. Depth profiles of ^{234}Th (black line), ^{238}U(black-dash line), Fluorescence (black-dotted line) and Dissolved Oxygen(grey-dash line)from surface to 300 m depth for all the stations.

Figure 6. Spatial variability of (a) primary production, (b) POC, (c) ^{234}Th flux, (d) POC/^{234}Th ratio, (e) POCexport flux (integratedup to 100 m depth) and (f) Th*E* ratioin the study region is shown. The grey discontinuous line shows the Equatorial Indian Ocean region. To bring out the variations in Th*E* values forall stations, though the y-axis ismarkedup to 0.1 and the high value of sta. 1 is written inside the corresponding bars of the histogram.

Figure 7. The relation between ^{234}Th flux and primary production in (a) the Indian Ocean and (b) the Bay of Bengal. Station numbers are provided along the symbols. A trend line is drawn for the stations to the south of equator. Sta. 9, located to the north of equator does not fall on this line. (c) The relation between ^{234}Th excess (inventory) and primary production in the Bay of Bengal is shown. The ^{234}Th flux and inventory of ^{234}Th excess with respect to ^{238}U activity are calculated from surface to 100 m depth.

Figure 8. Plot showing the relation between primary productionandPOC export flux at each station. Open circlesindicate the Bay of Bengal and the closed ones indicate the Indian Ocean. The corresponding stations numbers are given on topof each circle. The three trend lines represent 2 %, 5 % and 10 % POC export each. Stations 5, 6 & 11 are not shown in the figure as they showno POC export.

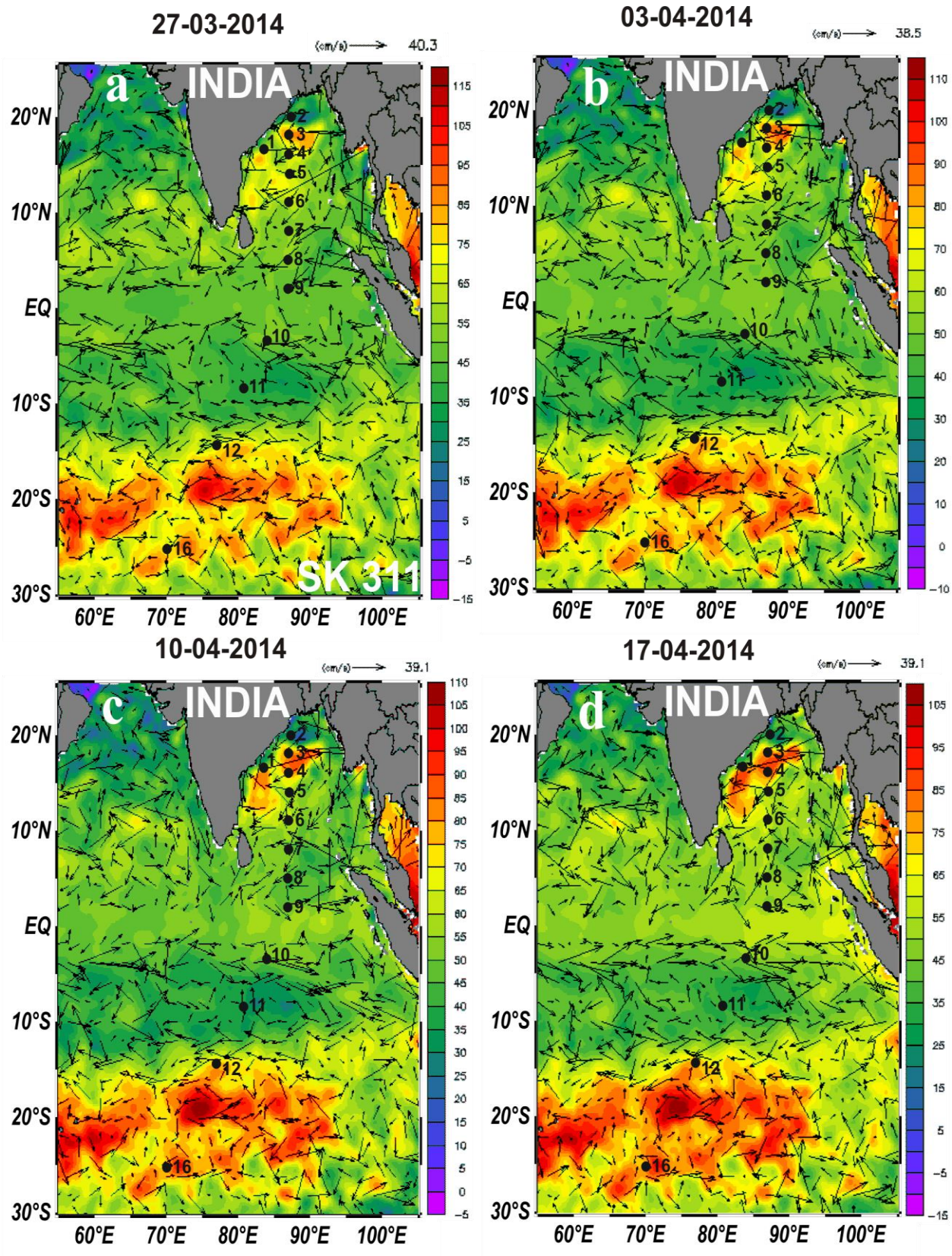
27-03-2014
(cm/s) 40.3
a
INDIA
SK 311
03-04-2014
(cm/s) 38.5
b
INDIA
10-04-2014
(cm/s) 39.1
c
INDIA
17-04-2014
(cm/s) 39.1
d
INDIA
20°N
10°N
EQ
10°S
20°S
30°S
60°E
70°E
80°E
90°E
100°E
Latitude
Longitude

Fig. 1

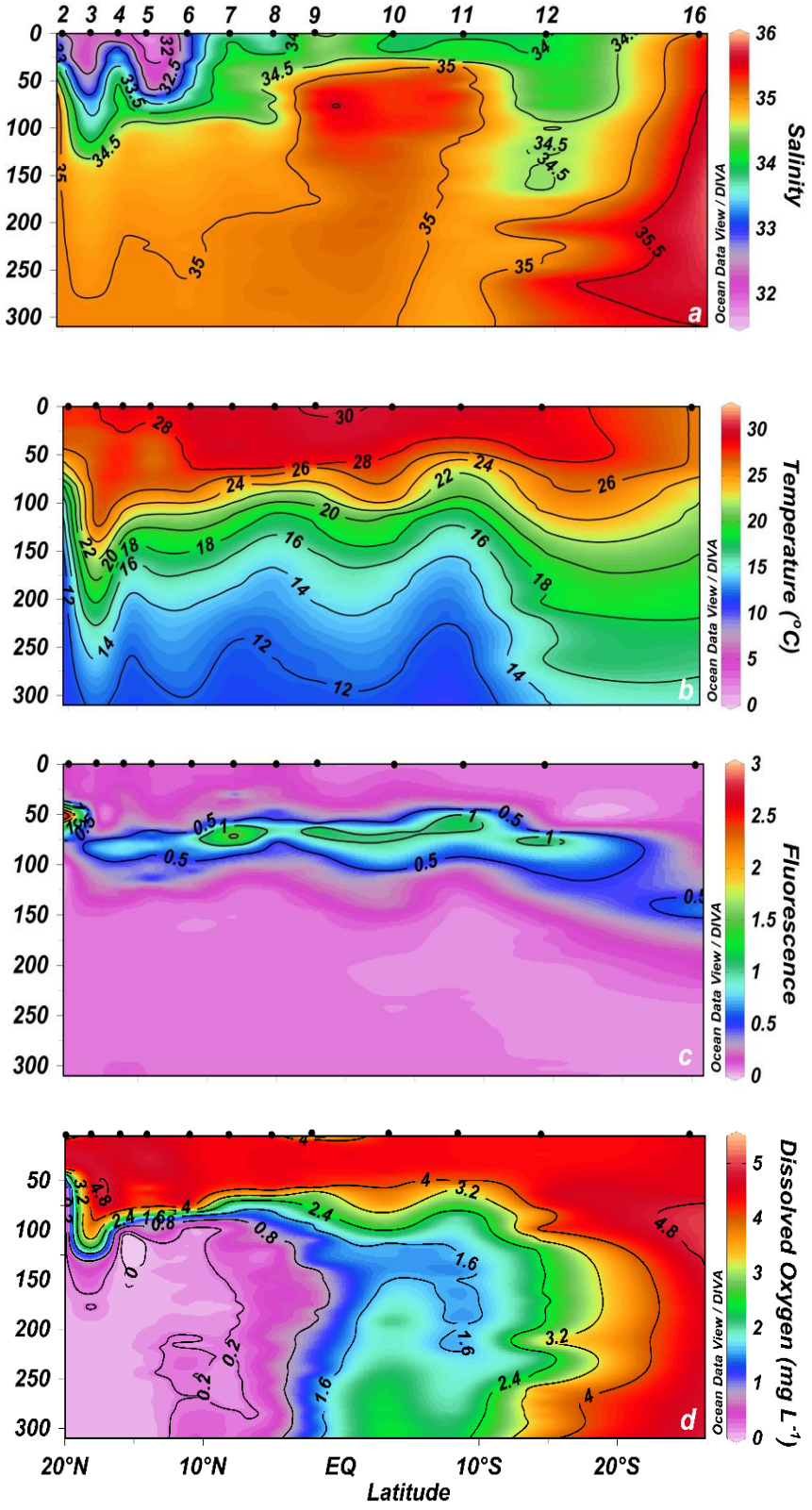
Depth (m)
Salinity
Temperature (°C)
Fluorescence
Dissolved Oxygen (mg L-1)
Ocean Data View / DIVA
a
b
c
d
20°N
10°N
EQ
10°S
20°S
Latitude

Fig. 2

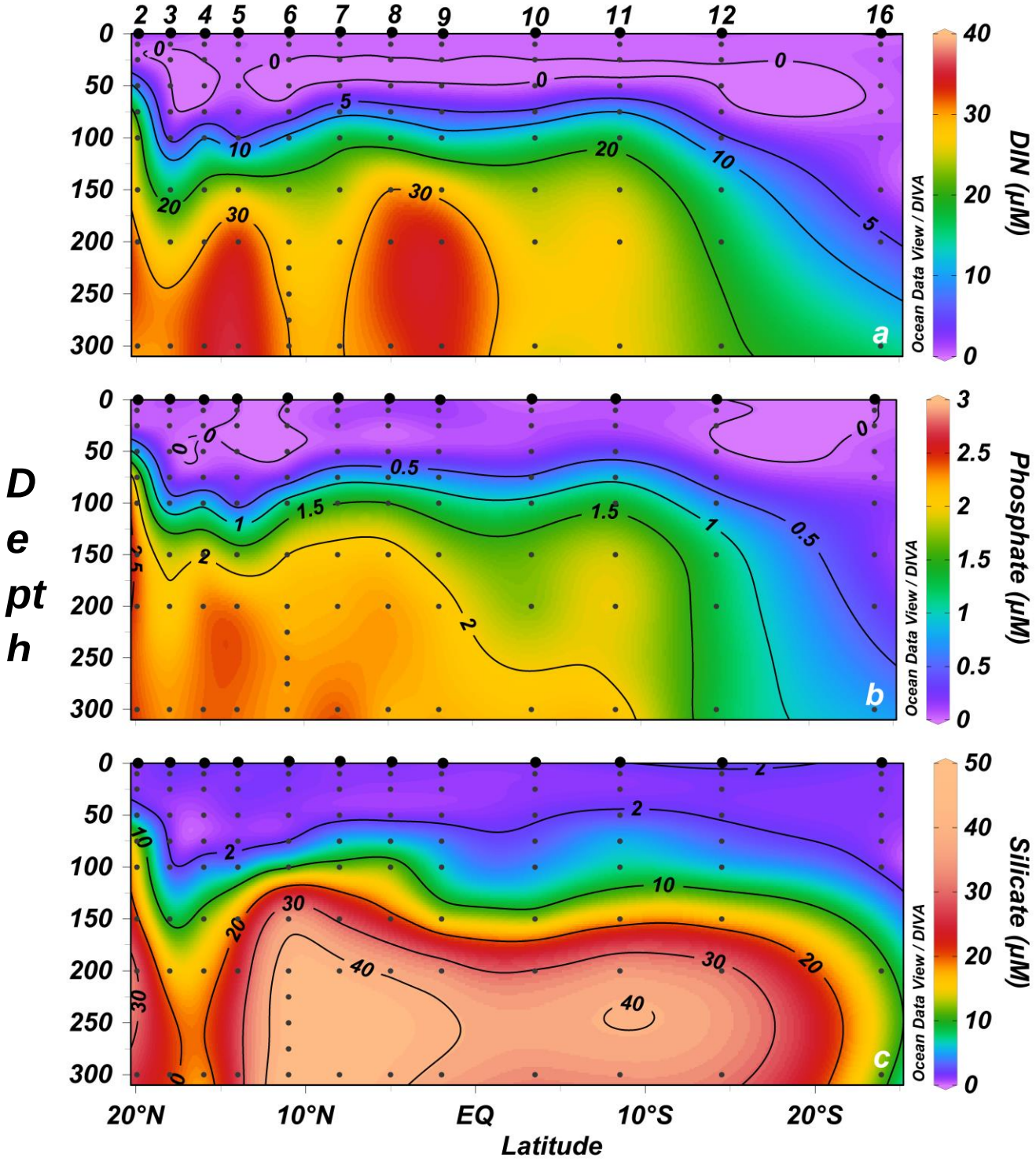
2 3 4 5 6 7 8 9 10 11 12 16
0 50 100 150 200 250 300
Depth
DIN (µM)
Phosphate (µM)
Silicate (µM)
Ocean Data View / DIVA
a
b
c
20°N 10°N EQ 10°S 20°S
Latitude

Fig.3

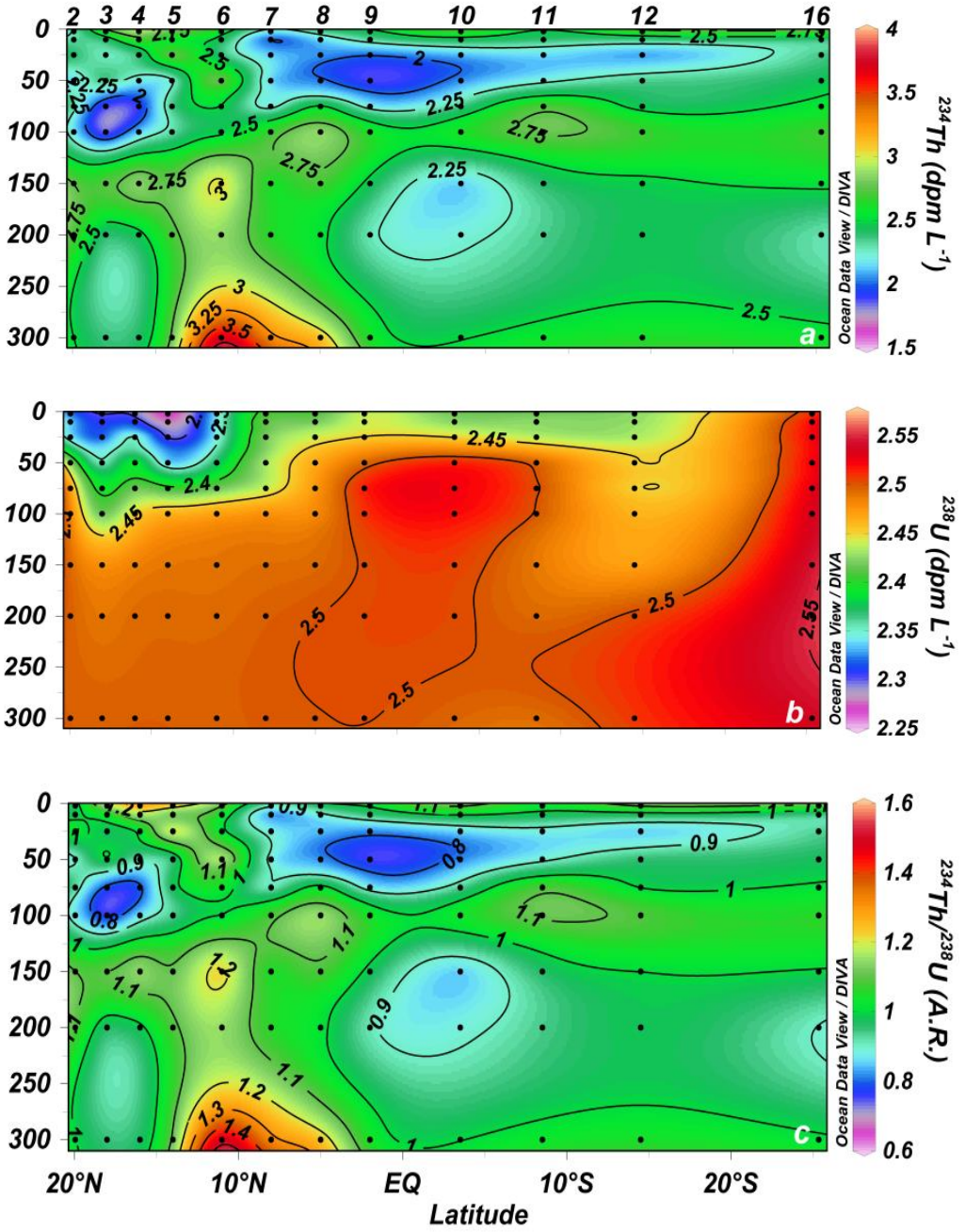
Depth (m)
Latitude
20°N
10°N
EQ
10°S
20°S
a
b
c
Ocean Data View / DIVA
234Th (dpm L-1)
238U (dpm L-1)
234Th/238U (A.R.)

Fig. 4

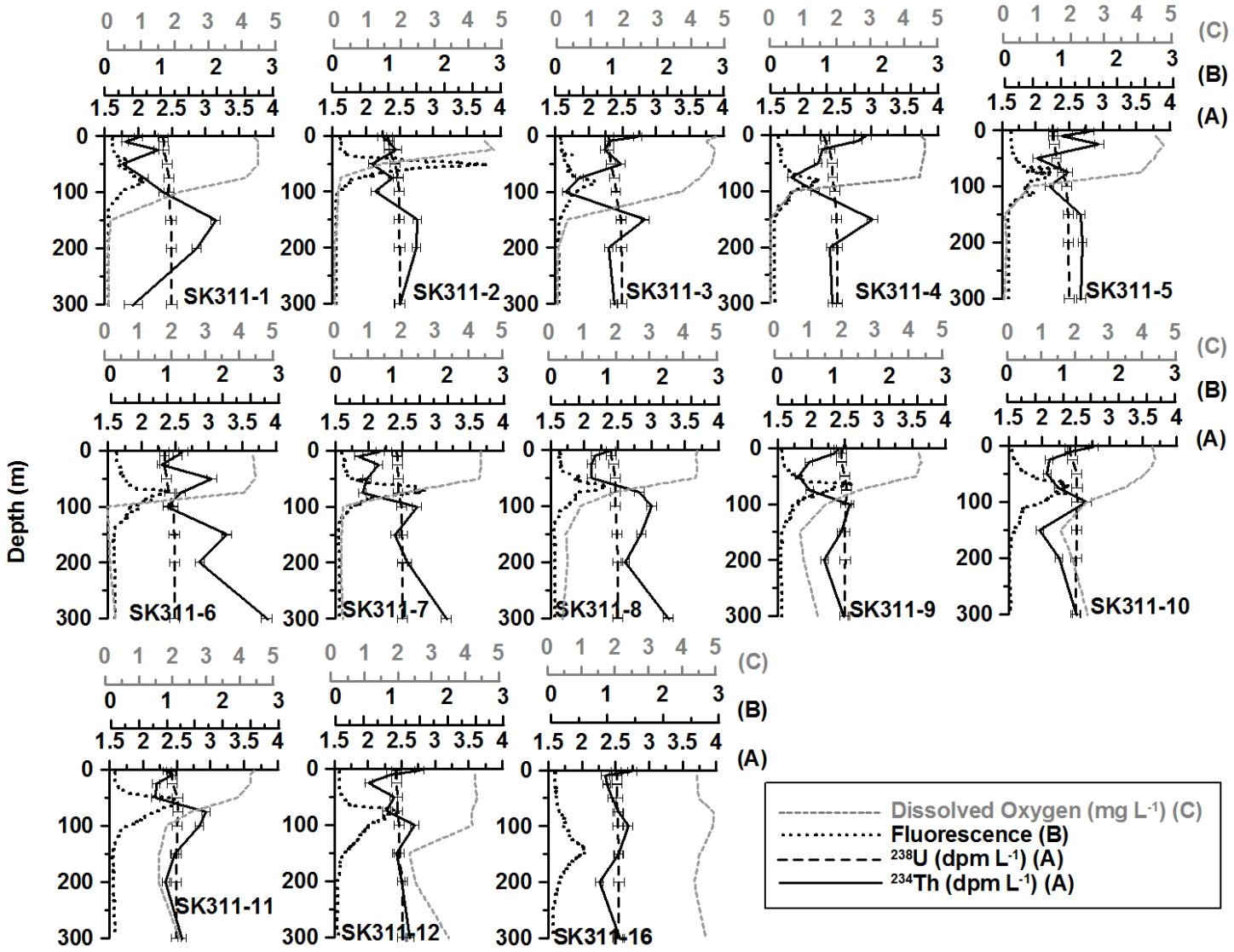
Depth (m)
SK311-1
SK311-2
SK311-3
SK311-4
SK311-5
SK311-6
SK311-7
SK311-8
SK311-9
SK311-10
SK311-11
SK311-12
SK311-16
(C)
(B)
(A)
Dissolved Oxygen (mg L-1) (C)
Fluorescence (B)
238U (dpm L-1) (A)
234Th (dpm L-1) (A)

Fig. 5

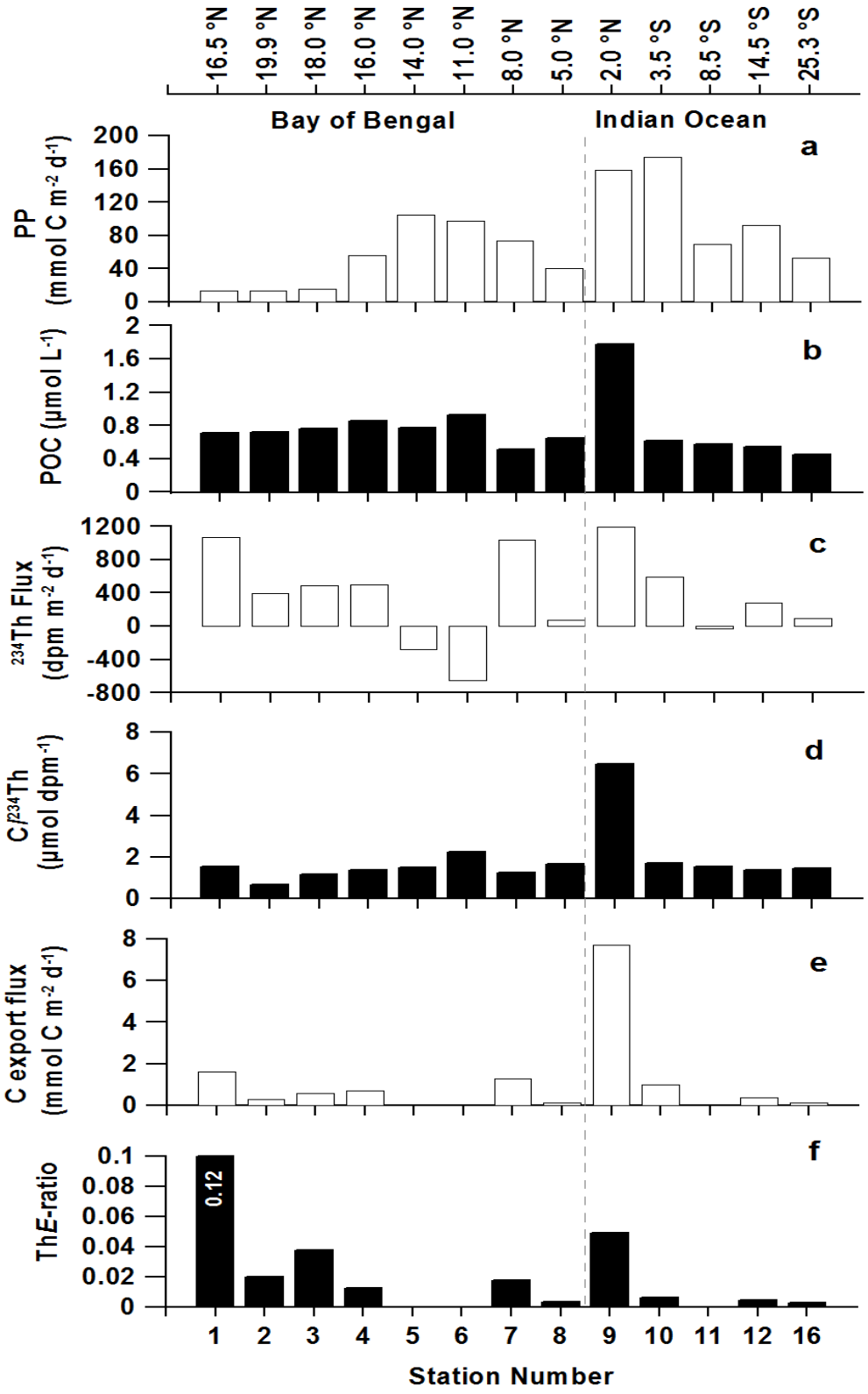
16.5 °N
19.9 °N
18.0 °N
16.0 °N
14.0 °N
11.0 °N
8.0 °N
5.0 °N
2.0 °N
3.5 °S
8.5 °S
14.5 °S
25.3 °S
Bay of Bengal
Indian Ocean
PP (mmol C m-2 d-1)
a
POC (µmol L-1)
b
234Th Flux (dpm m-2 d-1)
c
C/234Th (µmol dpm-1)
d
C export flux (mmol C m-2 d-1)
e
ThE-ratio
0.12
f
Station Number

Fig. 6

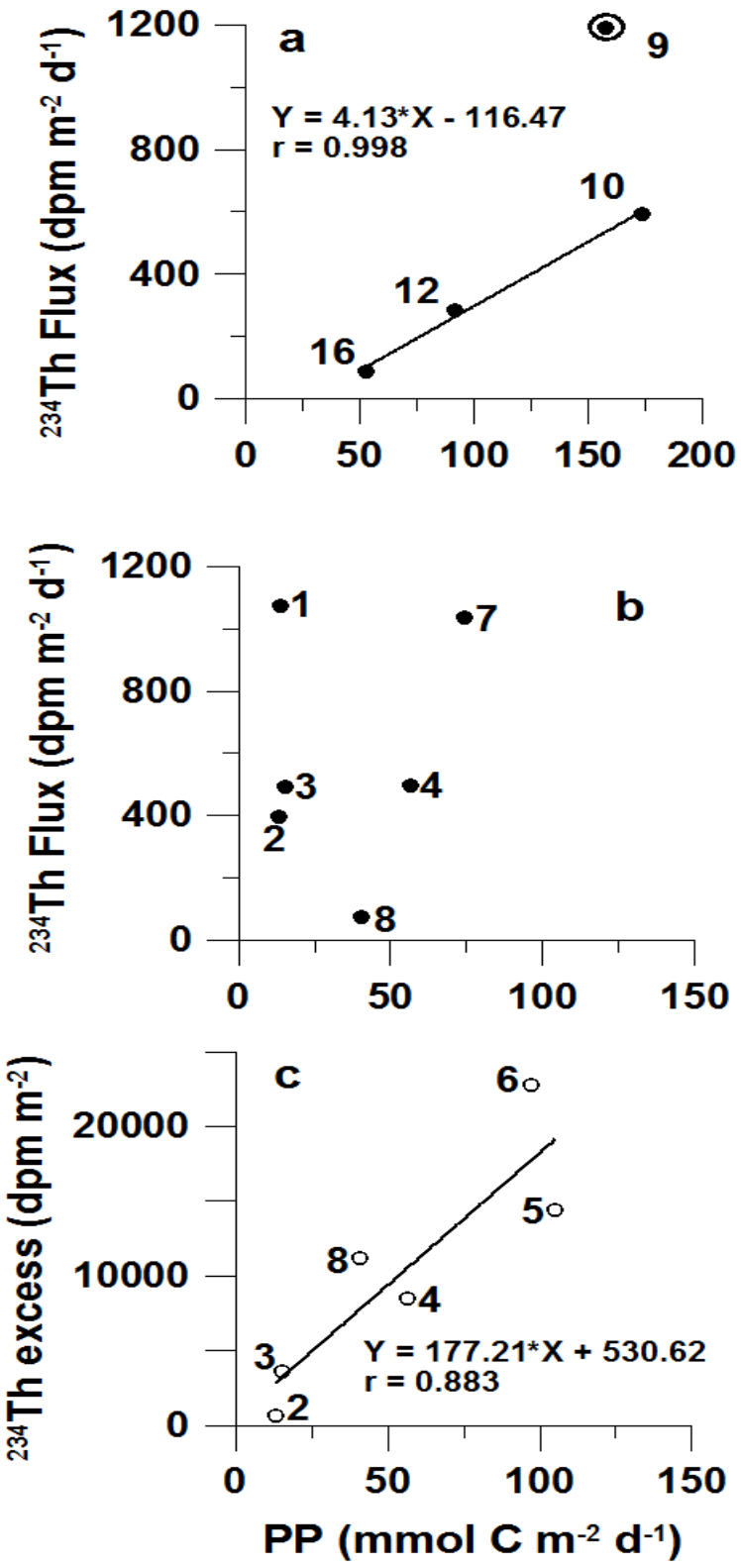
a
9
Y = 4.13*X - 116.47
r = 0.998
10
12
16
1200
800
400
0
0
50
100
150
200
234Th Flux (dpm m-2 d-1)
b
1
7
3
4
2
8
1200
800
400
0
0
50
100
150
234Th Flux (dpm m-2 d-1)
c
6
5
8
4
3
2
Y = 177.21*X + 530.62
r = 0.883
20000
10000
0
0
50
100
150
234Th excess (dpm m-2)
PP (mmol C m-2 d-1)

Fig. 7

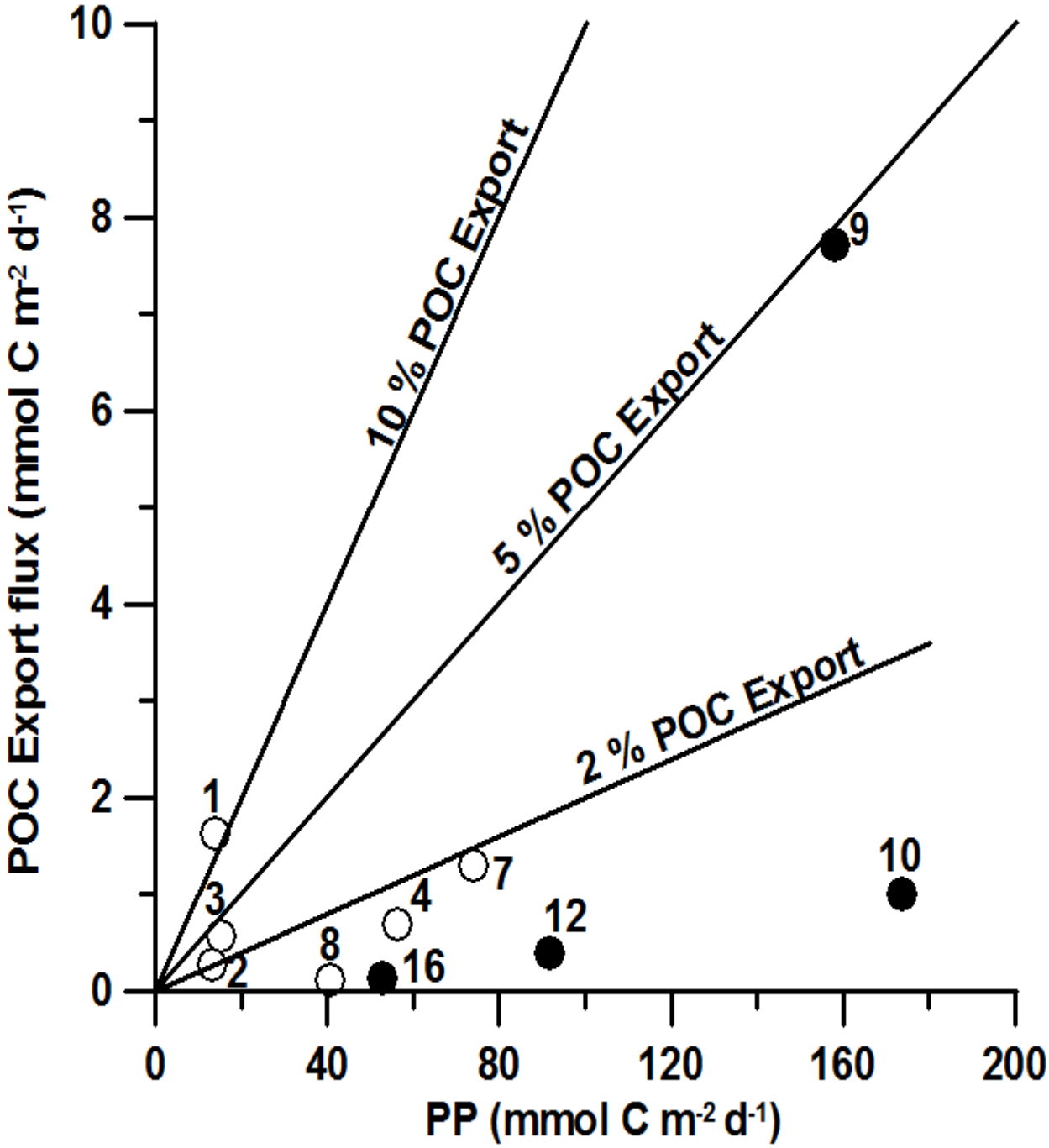
10 % POC Export
5 % POC Export
2 % POC Export
POC Export flux (mmol C m-2 d-1)
PP (mmol C m-2 d-1)
0
2
4
6
8
10
0
40
80
120
160
200
1
2
3
4
7
8
16
12
9
10

Fig. 8

Table 1

Station details (location, total water column depth and date of collection), depth, potential temperature, salinity, ^{238}U, total ^{234}Th and the total $^{234}Th/^{238}U$ ratio (A.R.) for the SK311 cruise. Standard deviations of radionuclide data are based on counting error (1σ).

Depth (m)	Pot. Temp. (ºC)	Salinity	^{238}U (dpm L^{-1})	^{234}Th (dpm L^{-1})	$^{234}Th/^{238}U$ (A.R.)
Sta. 1, 16º 32.02'N, 83º 34.03'E; 2900 m, 26.3.2014					
2	28.282	33.176	2.37±0.07	2.00±0.06	0.844±0.035
10	28.309	33.315	2.38±0.07	1.80±0.05	0.759±0.032
25	28.171	33.421	2.38±0.07	2.30±0.07	0.963±0.040
50	27.794	34.009	2.42±0.07	1.77±0.05	0.730±0.031
75	27.810	34.433	2.46±0.07	2.09±0.06	0.849±0.035
100	24.468	34.376	2.45±0.07	2.37±0.06	0.965±0.038
150	18.948	34.853	2.48±0.07	3.15±0.07	1.268±0.047
200	14.571	34.958	2.49±0.07	2.87±0.07	1.151±0.043
300	11.785	35.022	2.50±0.07	1.93±0.14	0.772±0.060
2000 A	2.441	34.768	2.48±0.07	2.49±0.06	1.005±0.038
2000 B	2.441	34.768	2.48±0.07	2.41±0.06	0.971±0.039
Sta. 2, 19º 56.67'N, 87º 17.73'E; 1079 m, 28.3.2014					
3	27.628	32.543	2.32±0.07	2.24±0.07	0.965±0.040
10	27.554	32.823	2.34±0.07	2.33±0.06	0.997±0.040
25	26.496	32.829	2.34±0.07	2.44±0.09	1.042±0.051
50	25.493	34.125	2.43±0.07	2.09±0.06	0.859±0.034
75	21.567	34.749	2.48±0.07	2.39±0.06	0.965±0.037
100	17.287	34.898	2.49±0.07	2.14±0.06	0.859±0.035
150	14.436	34.965	2.49±0.07	2.76±0.06	1.107±0.042
200	12.392	35.008	2.50±0.07	2.74±0.06	1.099±0.041
300	11.060	35.026	2.50±0.07	2.50±0.07	1.002±0.042
Sta. 3, 18º 0.896'N, 87º 0.029'E; 2502 m, 29.3.2014					
4	27.839	32.236	2.30±0.07	2.73±0.07	1.186±0.046
10	27.829	32.282	2.30±0.07	2.31±0.06	1.003±0.040
25	26.890	32.281	2.30±0.07	2.23±0.06	0.969±0.039
50	26.854	32.673	2.33±0.07	2.48±0.06	1.066±0.042
75	26.860	33.375	2.38±0.07	1.86±0.05	0.782±0.033
100	26.404	33.670	2.40±0.07	1.66±0.05	0.693±0.029
150	22.967	34.777	2.48±0.07	2.84±0.06	1.145±0.043
200	18.326	34.865	2.49±0.07	2.29±0.06	0.922±0.036
300	12.441	35.013	2.50±0.07	2.38±0.06	0.952±0.037

Sta. 4, 16º 0.185'N, 87º 0.014'E; 2816 m, 30.3.2014					
4	28.856	32.286	2.30±0.07	2.93±0.07	1.271±0.049
10	28.591	32.497	2.32±0.07	2.80±0.07	1.210±0.046
25	28.240	33.404	2.38±0.07	2.27±0.06	0.953±0.038
50	27.818	33.963	2.42±0.07	2.21±0.06	0.912±0.036
75	27.425	34.034	2.43±0.07	1.81±0.05	0.745±0.031
100	25.177	34.449	2.46±0.07	2.16±0.06	0.880±0.037
150	18.269	34.855	2.49±0.07	3.02±0.08	1.215±0.049
200	14.185	34.963	2.49±0.07	2.39±0.06	0.958±0.037
300	11.581	35.027	2.50±0.07	2.42±0.06	0.970±0.038
Sta. 5, 14º 0.21'N, 87º 0.06'E; 3094 m, 31.3.2014					
4	28.399	31.718	2.26±0.07	2.80±0.07	1.237±0.049
10	28.142	31.802	2.27±0.07	2.40±0.16	1.056±0.075
25	27.519	31.965	2.28±0.07	2.95±0.07	1.294±0.050
50	26.285	32.439	2.31±0.07	2.02±0.06	0.873±0.036
75	26.636	33.624	2.40±0.07	2.48±0.07	1.036±0.041
100	24.004	34.590	2.47±0.07	2.21±0.06	0.894±0.037
150	17.841	34.883	2.49±0.07	2.67±0.06	1.072±0.041
200	14.194	34.960	2.49±0.07	2.70±0.06	1.084±0.041
300	11.627	35.026	2.50±0.07	2.68±0.07	1.072±0.042
Sta. 6, 11º 0.78'N, 87º 0.02'E; 3450 m, 01.4.2014					
4	29.193	32.831	2.34±0.07	2.62±0.07	1.120±0.044
10	29.189	32.852	2.34±0.07	2.54±0.07	1.082±0.043
25	29.062	32.834	2.34±0.07	2.30±0.06	0.981±0.039
50	28.522	33.279	2.37±0.07	3.05±0.07	1.283±0.049
75	26.981	33.866	2.41±0.07	2.59±0.06	1.071±0.042
100	23.941	34.689	2.47±0.07	2.38±0.06	0.961±0.037
150	17.870	34.887	2.49±0.07	3.27±0.07	1.315±0.049
200	14.239	34.956	2.49±0.07	2.86±0.07	1.149±0.043
300	11.961	35.008	2.50±0.07	3.86±0.08	1.548±0.057
2000	2.520	34.770	2.48±0.07	2.57±0.06	1.036±0.040
Sta. 7, 8º 1.02'N, 86º 59.93'E; 3768 m, 03.4.2014					
4	29.604	33.825	2.41±0.07	2.16±0.06	0.896±0.037
10	29.162	34.015	2.43±0.07	1.85±0.06	0.762±0.032
25	28.951	34.066	2.43±0.07	2.14±0.06	0.881±0.037
50	28.989	34.204	2.44±0.07	1.97±0.06	0.808±0.034
75	25.162	34.097	2.43±0.07	1.90±0.05	0.783±0.032
100	21.839	34.852	2.48±0.07	2.72±0.06	1.093±0.042
150	16.348	34.955	2.49±0.07	2.39±0.06	0.959±0.038
200	13.491	35.019	2.50±0.07	2.57±0.06	1.028±0.040
300	11.261	35.041	2.50±0.07	3.15±0.07	1.261±0.048
Sta. 8, 5º 0.56'N, 86º 59.75'E; 4106 m, 04.4.2014					
4	29.466	33.630	2.40±0.07	2.40±0.07	0.999±0.040

10	29.469	33.712	2.40±0.07	2.17±0.06	0.904±0.037
25	29.302	34.162	2.44±0.07	2.11±0.06	0.866±0.036
50	28.950	34.516	2.46±0.07	2.10±0.06	0.854±0.036
75	25.125	34.595	2.47±0.07	2.82±0.08	1.144±0.046
100	19.656	34.611	2.47±0.07	3.01±0.07	1.219±0.047
150	14.859	34.937	2.49±0.07	2.85±0.07	1.144±0.044
200	13.014	35.061	2.50±0.07	2.61±0.06	1.044±0.040
300	11.444	35.052	2.50±0.07	3.25±0.08	1.301±0.049
Sta. 9, 2º 0.41'N, 87º 0.03'E; 4449 m, 06.4.2014					
2	30.237	34.342	2.45±0.07	2.40±0.06	0.982±0.039
10	29.842	34.406	2.45±0.07	2.35±0.06	0.956±0.038
25	29.780	34.357	2.45±0.07	1.96±0.06	0.801±0.033
50	28.887	34.977	2.49±0.07	1.81±0.05	0.725±0.030
75	24.257	35.404	2.52±0.07	1.98±0.06	0.783±0.032
100	20.926	35.274	2.52±0.07	2.57±0.06	1.020±0.039
150	16.166	35.059	2.50±0.07	2.45±0.06	0.980±0.038
200	14.147	35.107	2.50±0.07	2.19±0.06	0.876±0.034
300	11.663	35.072	2.50±0.07	2.49±0.06	0.996±0.038
Sta. 10, 3º 30.04'S, 84º 0.03'E; 5005 m, 08.4.2014					
4	29.748	33.822	2.41±0.07	2.77±0.07	1.146±0.044
10	29.555	33.895	2.42±0.07	2.44±0.06	1.009±0.039
25	29.593	34.344	2.45±0.07	2.10±0.05	0.859±0.034
50	27.939	35.272	2.51±0.07	2.07±0.05	0.824±0.033
75	25.979	35.304	2.52±0.07	2.24±0.06	0.891±0.035
100	23.448	35.330	2.52±0.07	2.67±0.06	1.058±0.041
150	16.885	35.175	2.51±0.07	1.96±0.06	0.783±0.032
200	13.990	35.130	2.50±0.07	2.25±0.06	0.898±0.035
300	11.576	35.014	2.50±0.07	2.51±0.06	1.004±0.038
2000	2.5976	34.766	2.48±0.07	2.53±0.07	1.021±0.041
Sta. 11, 8º 29.9'S, 80º 48.12'E; 5281 m, 11.4.2014					
4	29.497	33.938	2.42±0.07	2.35±0.06	0.972±0.038
10	29.291	34.139	2.43±0.07	2.42±0.06	0.993±0.038
25	28.841	34.139	2.43±0.07	2.19±0.05	0.901±0.035
50	25.494	35.182	2.51±0.08	2.18±0.06	0.870±0.034
75	21.475	35.225	2.51±0.08	2.93±0.06	1.167±0.043
100	18.893	35.146	2.51±0.08	2.83±0.07	1.131±0.043
150	14.354	34.913	2.49±0.07	2.47±0.06	0.990±0.038
200	12.654	34.916	2.49±0.07	2.34±0.06	0.938±0.036
300	10.949	34.908	2.49±0.07	2.58±0.06	1.035±0.039
Sta. 12, 14º 29.46'S, 76º 59.69'E; 5281 m, 13.4.2014					
4	28.779	34.000	2.42±0.07	2.77±0.07	1.141±0.044
10	28.782	33.977	2.42±0.07	2.34±0.06	0.965±0.038
25	28.779	34.043	2.43±0.07	2.01±0.06	0.828±0.034
50	28.584	34.226	2.44±0.07	2.38±0.06	0.976±0.038

75	25.729	34.161	2.44±0.07	2.27±0.06	0.934±0.037
100	24.355	34.445	2.46±0.07	2.69±0.06	1.097±0.042
150	19.903	34.492	2.46±0.07	2.42±0.06	0.985±0.038
200	17.974	35.177	2.51±0.08	2.49±0.06	0.995±0.038
300	13.903	35.210	2.51±0.08	2.62±0.06	1.045±0.040
Sta. 16, 25º 19.20'S, 70º 2.43'E; 2442 m, 19.4.2014					
4	25.904	35.197	2.51±0.08	2.75±0.07	1.094±0.043
10	25.916	35.357	2.52±0.08	2.35±0.06	0.932±0.036
25	25.905	35.400	2.52±0.08	2.37±0.06	0.938±0.037
50	25.873	35.416	2.53±0.08	2.45±0.06	0.972±0.038
75	23.870	35.487	2.53±0.08	2.55±0.07	1.008±0.040
100	22.206	35.571	2.54±0.08	2.69±0.07	1.061±0.041
150	20.249	35.711	2.55±0.08	2.55±0.06	1.001±0.038
200	18.475	35.772	2.55±0.08	2.26±0.06	0.887±0.034
300	15.384	35.566	2.54±0.08	2.57±0.06	1.012±0.039
2000	2.185	34.703	2.47±0.07	2.57±0.07	1.037±0.041

Table 2

^{238}U, total ^{234}Th and $^{234}Th/^{238}U$ (A.R.) of the samples collected at 2000 m depth from stations of SK311cruise. The Standard deviations of radionuclide data are based on counting error (1σ).

Sample code	**^{238}U (dpm L^{-1})**	**^{234}Th (dpm L^{-1})**	**$^{234}Th/^{238}U$ (AR)**
SK311/1/2000 M-A	2.48±0.07	2.49±0.06	1.00±0.04
SK311/1/2000 M-B	2.48±0.07	2.41±0.06	0.97±0.04
SK311/6/2000 M	2.48±0.07	2.57±0.06	1.04±0.04
SK311/10/2000 M	2.48±0.07	2.53±0.06	1.02±0.04
SK311/16/2000 M	2.47±0.07	2.57±0.06	1.04±0.04

Table 3.

Primary production, POC/^{234}Th ratio, POC-export fluxandTh*E* ratio for all the stations sampled in the SK311 cruise. Also shown are the POC export flux calculated using the empirical relationships provided by Laws et al. (2000, 2011), Dunne et al.(2005) and Henson et al. (2011).

Stn. No.	**Latitude**	**Longitude**	**In situ PP (mmol C m^{-2} d^{-1})**	**POC (µmol L^{-1})**	**^{234}Th (dpm L^{-1})**	**POC/ ^{234}Th [a] (µmol dpm^{-1})**	**^{234}Th Export Flux (dpm m^{-2} d^{-1}) [b]**	**POC Export Flux (mmol C m^{-2} d^{-1})**				**Th*E* ratio (%)**
								Laws model[c]	**Dunne model[c]**	**Henson model[c]**	**^{234}Th based**	
1	16º 32.020’N	83º 34.03’E	13.9	0.71	0.465	1.52	1072	1.2	2.3	0.3	1.6	11.7
2	19º 56.670’N	87º 17.73’E	13.2	0.72	1.06	0.69	395	1.1	2.6	0.3	0.3	2.1
3	18º 0.896’N	87º 0.029’E	15.2	0.76	0.659	1.15	492	1.4	2.7	0.4	0.6	3.7
4	16º 0.185’N	87º 0.014’E	56.3	0.85	0.613	1.39	499	7.3	13.8	1.3	0.7	1.2
5	14º 0.210’N	87º 0.06’E	105.1	0.78	0.517	1.50	(278)	16.7	30.0	2.5	-	-
6	11º 0.780’N	87º 0.02’E	97.1	0.93	0.417	2.23	(657)	14.6	27.0	2.2	-	-
7	8º 1.020’N	86º 59.93’E	74.1	0.51	0.407	1.26	1035	10.1	19.2	1.6	1.3	1.8
8	5º 0.560’N	86º 59.75’E	40.6	0.65	0.385	1.68	73	4.6	9.3	0.9	0.1	0.3
9	2º 0.410’N	87º 0.03’E	158.0	1.78	0.274	6.48	1192	26.4	47.8	3.2	7.7	4.9
10	3º 30.040’S	84º 0.03’E	173.8	0.61	0.362	1.70	594	30.5	53.3	3.7	1.0	0.6

11	8º 29.900’S	80º 48.12’E	69.3	0.57	0.376	1.52	(29)	9.3	18.2	1.5	-	-
12	14º 29.460’S	76º 59.69’E	91.8	0.54	0.389	1.39	282	13.8	25.4	2.1	0.4	0.4
16	25º 19.200’S	70º 2.43’E	52.8	0.45	0.304	1.47	88	7.4	12.7	1.5	0.1	0.2

[a]Particulates measured at 200 m depth.
[b]Integrated upto 100 m depth. Values in parentheses are excess ^{234}Th released from biological remineralization of sinking particulate material.
[c] In the model export calculations, in situ PP, surface temperature are used. Deep chlorophyll maximum (DCM) + 10 m is used for the depth of euphotic zone (Haskell II et al., 2015).